

# Low Cost Direction Finding with the Electronically Steerable Parasitic Array Radiator (ESPAR) Antenna

Jonathan Michael Berger

A dissertation submitted to the Faculty of Engineering and the Built Environment, University of the Witwatersrand, Johannesburg, South Africa in fulfilment of the requirements for the degree of Master of Science in Engineering.

Johannesburg, March 2005

# Declaration

I declare that this is my own, unaided work, except where otherwise acknowledged. It is being submitted for the degree of Master of Science in Engineering at the University of the Witwatersrand, Johannesburg, South Africa. It has not been submitted before for any degree or examination at any other university.

Signed this \_\_\_\_\_ day of \_\_\_\_\_ 2005

---

Jonathan Michael Berger

# Abstract

In this paper, the Electronically Steerable Parasitic Array Radiator (ESPAR) antenna, developed by the Advanced Telecommunications Research Institute (ATR) in Japan was analyzed to determine its feasibility as a low cost direction finding (DF) system. Simulations of the antenna were performed in SuperNEC and Matlab was used to determine the direction of arrival (DOA) using the Reactance Domain multiple signal classification (MUSIC) algorithm. Results show the ideal configuration has 6 parasitic elements with a diameter of  $0.5\lambda$ . Up to 5 periodic, uncorrelated signals spread  $360^\circ$  in azimuth and above  $45^\circ$  elevation produce sharp peaks in the MUSIC spectra. Azimuth separations of only  $2^\circ$  at 40 dB are resolvable while signals arriving with 25% full power are still detectable. For the DOA to be resolved the radiation pattern should be asymmetrical and hence the reactance set should have a range of unequal values. Comparative results show that the 6 element ESPAR offers excellent overall performance despite the reduction in cost and is comparable in performance to the 6 element uniform linear array.

# Acknowledgements

I wish to thank the following people for their contributions to this MSc research project:

*Prof. Alan Clark*, School of Electrical and Information Engineering, Electromagnetics Department, University of the Witwatersrand, Johannesburg. For his invaluable encouragement, support and guidance throughout this work.

*ARMSCOR*, The Armaments Corporation of South Africa. For providing financial support making this research possible.

*Mom, Dad, David & Mark*

*Karen*

# Foreword

This dissertation is presented to the University of the Witwatersrand, Johannesburg, South Africa for the degree of Master of Science in Engineering.

The dissertation is entitled “Low Cost Direction Finding with the Electronically Steerable Parasitic Array Radiator (ESPAR) Antenna.” In this study, research was undertaken to explore methods and techniques of Direction Finding (DF) antennas and Direction Finding resolution algorithms. Although research has been done on Direction Finding in the past, this study focuses on low cost implementations of DF antennas and algorithms. The ESPAR antenna is presented together with the Reactance Domain multiple signal classification (MUSIC) algorithm as a possible solution for low cost high performance DF systems. The antenna is simulated in SuperNEC and the algorithm simulated in Matlab. The results are presented in terms of DF performance and compared to conventional expensive methods.

This document complies with the university’s so-called ‘paper model’ format, and although the actual paper contains the essence of the research, the appendices present aspects of the work that are not covered in great detail in the main document.

*Appendix A* contains all the simulation results from SuperNEC for the ESPAR antenna and Reactance domain MUSIC algorithm.

*Appendix B* details simulation results that show a direction finding performance comparison between the ESPAR antenna and the conventional uniform linear array.

*Appendix C* introduces the SuperNEC command files written in Matlab to simulate the antennas and is stored on the attached CD.

# Table of Contents

|   |             |
|---|-------------|
| <b>Abstract</b>   | <b>iii</b>  |
| <b>Acknowledgements</b>   | <b>iv</b>   |
| <b>Foreword</b>   | <b>v</b>    |
| <b>Table of Contents</b>  | <b>vi</b>   |
| <b>List of Figures</b>  | <b>viii</b> |
| <b>List of Tables</b>   | <b>ix</b>   |
| <b>Paper: Low Cost Direction Finding with the Electronically Steerable Parasitic Array Radiator (ESPAR) Antenna</b> | <b>1</b>    |
| <b>I. Introduction</b>  | <b>1</b>    |
| <b>II. Applications of Direction Finding</b>  | <b>1</b>    |
| <b>III. Parasitic Antenna Overview</b>  | <b>1</b>    |
| A. Initial Work .....   | 1           |
| B. Advantages of Parasitic Antennas .....   | 2           |
| C. Configurations of the Parasitic Antenna.....   | 2           |
| D. Direction Finding Techniques for Parasitic Antennas.....   | 2           |
| <b>IV. The ESPAR Antenna</b>  | <b>2</b>    |
| A. Basic Configuration .....  | 2           |
| B. Signal Model .....   | 3           |
| <b>V. Reactance Domain MUSIC Algorithm</b>  | <b>3</b>    |
| A. Single-Port Correlation Matrix.....  | 3           |
| B. Reactance Domain MUSIC .....   | 3           |
| <b>VI. ESPAR Simulations</b>  | <b>4</b>    |
| A. Number of Parasitic Elements .....   | 4           |
| B. ESPAR Diameter .....   | 4           |
| C. Performance of the Reactance Domain MUSIC Algorithm .....  | 5           |
| 1) Snapshots .....  | 5           |
| 2) Additive Noise .....   | 5           |
| 3) Number of Resolvable Signals .....   | 5           |
| 4) Periodicity of Incoming Signals .....  | 5           |
| 5) Signal Separation .....  | 5           |
| 6) Signals having different Power Levels.....   | 5           |
| 7) Load Reactances.....   | 5           |
| 8) Azimuth & Elevation Coverage .....   | 6           |
| 9) Frequency Response.....  | 6           |
| 10) Speed of DOA Estimation.....  | 6           |
| 11) Performance in a Correlated Noise Environment.....  | 6           |
| D. Statistical Analysis .....   | 7           |
| <b>VII. Construction &amp; Testing</b>  | <b>7</b>    |
| <b>VIII. Performance Comparison to Expensive Methods</b>  | <b>7</b>    |

|  |           |
|--|-----------|
| <b>IX. Conclusions</b>   | <b>7</b>  |
| <b>X. References</b>   | <b>8</b>  |
| <b>Appendix A: ESPAR Antenna Simulation Results</b>                                  | <b>9</b>  |
| A. Introduction.....   | 9         |
| B. The SuperNEC Model.....   | 9         |
| C. Number of Elements.....   | 9         |
| 1) 3 Element ESPAR Antenna.....  | 10        |
| 2) 5 Element ESPAR Antenna.....  | 10        |
| 3) 6 Element ESPAR Antenna.....  | 11        |
| 4) 7 Element ESPAR Antenna.....  | 11        |
| 5) Comparisons of Number of Elements.....  | 12        |
| D. ESPAR Diameter.....   | 12        |
| E. Reactance Music.....  | 15        |
| 1) Snapshots.....  | 15        |
| 2) Signal to Noise Ratio.....  | 16        |
| 3) Signal Separation.....  | 16        |
| 4) Different Power Levels.....   | 17        |
| 5) Azimuth & Elevation Coverage.....   | 18        |
| F. Statistical Analysis.....   | 19        |
| G. Load Reactances.....  | 20        |
| H. Conclusion.....   | 26        |
| I. References.....   | 26        |
| <b>Appendix B: Uniform Linear Array and ESPAR Performance Comparison Simulations</b> | <b>27</b> |
| A. Introduction.....   | 27        |
| B. Azimuth Coverage.....   | 27        |
| C. Elevation Capability.....   | 28        |
| D. Signal separation.....  | 29        |
| E. Conclusion.....   | 29        |
| F. References.....   | 29        |
| <b>Appendix C: Software Code and Output Files</b>                                    | <b>30</b> |
| A. Introduction.....   | 30        |
| B. The Simulation Files.....   | 30        |
| C. The Steering Vectors.....   | 31        |
| D. Conclusion.....   | 33        |

# List of Figures

|    |   |    |
|----|---|----|
| 1  | The configuration of the ESPAR antenna .....  | 2  |
| 2  | The formation of the correlation matrix in Reactance Domain MUSIC .....                                   | 3  |
| 3  | MUSIC spectra for ESPAR antennas of different number of elements .....                                    | 4  |
| 4  | Radiation patterns for ESPAR of various diameters .....   | 4  |
| 5  | Smith chart of impedance for increasing ESPAR diameter.....   | 4  |
| 6  | Reactance MUSIC spectra for various numbers of snapshots.....   | 5  |
| 7  | Reactance Music spectra for various signal-to-noise ratios .....  | 5  |
| 8  | Angular resolution limits for various signal-to-noise ratios .....  | 5  |
| 9  | Radiation pattern for various load combinations.....  | 6  |
| 10 | Reactance MUSIC spectra for various elevation angles.....   | 6  |
| 11 | Statistical analysis of Reactance MUSIC spectra for 250 trials .....                                      | 7  |
| 12 | The SuperNEC model of the ESPAR antenna.....  | 9  |
| 13 | Reactance MUSIC spectra for various signal-to-noise ratios for the three element ESPAR.....               | 10 |
| 14 | Reactance MUSIC spectra for various signal-to-noise ratios for the five element ESPAR .....               | 10 |
| 15 | Reactance MUSIC spectra for various signal-to-noise ratios for the six element ESPAR.....                 | 11 |
| 16 | Reactance MUSIC spectra for various signal-to-noise ratios for the seven element ESPAR .....              | 11 |
| 17 | Reactance MUSIC spectra for 3, 5, 6, & 7 element ESPAR antennas at SNR=20dB.....                          | 12 |
| 18 | Reactance MUSIC spectra for various ESPAR diameters .....   | 13 |
| 19 | Reactance MUSIC spectra for $0.4\lambda$ , $0.5\lambda$ and $0.6\lambda$ ESPAR diameters .....            | 13 |
| 20 | Smith chart for the ESPAR of diameters $0.25\lambda$ - $0.5\lambda$ .....                                 | 14 |
| 21 | Radiation patterns for $0.25\lambda$ to $0.5\lambda$ diameter ESPAR configurations.....                   | 14 |
| 22 | Reactance MUSIC spectra resolving 2 signals at 20dB SNR for 50, 250, 500 and 1000 snapshots .....         | 15 |
| 23 | Reactance MUSIC spectra resolving 2 signals at 20dB SNR for 10, 50, 100 and 200 snapshots .....           | 15 |
| 24 | Reactance MUSIC spectra for SNR of 0, 10, 20 and 30 dB.....   | 16 |
| 25 | Reactance MUSIC spectra with 1000 snapshots and various SNR for azimuth separation of $1^\circ$ .....     | 16 |
| 26 | Reactance MUSIC spectra with 1000 snapshots and various SNR for azimuth separation of $0.5^\circ$ .....   | 17 |
| 27 | Reactance MUSIC spectra with 1000 snapshots and various SNR for azimuth separation of $0.2^\circ$ .....   | 17 |
| 28 | Reactance MUSIC spectra for signals impinging with various power levels.....                              | 18 |
| 29 | Reactance MUSIC spectra with five signals dispersed over $360^\circ$ azimuth.....                         | 18 |
| 30 | Reactance MUSIC spectra for elevation angles of $15^\circ$ , $25^\circ$ , $45^\circ$ and $90^\circ$ ..... | 19 |
| 31 | Statistical analysis of Reactance MUSIC spectra with 250 iterations .....                                 | 19 |
| 32 | Reactance MUSIC spectra for Inductive, Capacitive and MaxMin Load reactance sets .....                    | 20 |
| 33 | Radiation pattern for load reactance sets Inductive, Capacitive and MinMax .....                          | 21 |
| 34 | Reactance MUSIC spectra for loads sets Random1, Random2 and Random3.....                                  | 21 |
| 35 | Radiation pattern for load reactance sets Random1, Random2 & Random3 .....                                | 22 |
| 36 | Reactance MUSIC spectra for loads sets Random4, Random5 and Random6.....                                  | 22 |
| 37 | Radiation pattern for load reactance sets Random4, Random5 & Random6 .....                                | 23 |
| 38 | Reactance MUSIC spectra for loads sets Optimised, Random4 & Limited25 .....                               | 23 |
| 39 | Radiation pattern for load reactance set Optimised, Random4 & Limited25.....                              | 24 |
| 40 | VSWR response of the ESPAR antenna for reactance sets Random1, Random2, Random3 and Random4. ....         | 24 |
| 41 | VSWR response of the ESPAR antenna for reactance sets Random4, Random5, Random6 and Optimised. ....       | 25 |
| 42 | VSWR response of the ESPAR antenna for reactance sets Optimised, MaxMin, Inductive and Capacitive.....    | 25 |
| 43 | Combined MUSIC spectra for 6 element ESPAR and ULA over full azimuth.....                                 | 27 |
| 44 | Combined MUSIC spectra for the ESPAR and ULA over $180^\circ$ .....                                       | 28 |
| 45 | Combined MUSIC spectra for ESPAR and ULA for various elevation angles .....                               | 28 |
| 46 | Combined MUSIC spectra for ESPAR and ULA for narrow azimuth separation .....                              | 29 |



# List of Tables

|     |   |    |
|-----|---|----|
| I   | Direction Finding Applications .....                | 1  |
| II  | ESPAR Design Parameters .....                       | 3  |
| III | ESPAR Load Reactances .....                         | 6  |
| IV  | Comparison of the ESPAR to the ULA.....             | 7  |
| V   | Load reactance sets used for the optimisation ..... | 20 |

# Low Cost Direction Finding with the Electronically Steerable Parasitic Array Radiator (ESPAR) Antenna

JONATHAN MICHAEL BERGER

**Abstract** – In this paper, the Electronically Steerable Parasitic Array Radiator (ESPAR) antenna, developed by the Advanced Telecommunications Research Institute (ATR) in Japan, was analyzed to determine its feasibility as a low cost direction finding (DF) system. Simulations of the antenna were performed in SuperNEC and Matlab was used to determine the direction of arrival (DOA) using the Reactance Domain multiple signal classification (MUSIC) algorithm. Results show the ideal configuration has 6 parasitic elements with a diameter of  $0.5\lambda$ . Up to 5 periodic, uncorrelated signals spread  $360^\circ$  in azimuth and above  $45^\circ$  elevation produce sharp peaks in the MUSIC spectra. Azimuth separations of only  $2^\circ$  at 40 dB are resolvable while signals arriving with 25% full power are still detectable. For the DOA to be resolved the radiation pattern should be asymmetrical and hence the reactance set should have a range of unequal values. Comparative results show that the 6 element ESPAR offers excellent overall performance despite the reduction in cost and is comparable in performance to the 6 element uniform linear array.

## I. INTRODUCTION

The number of mobile phone subscribers is growing annually so the demand for more efficient use of the frequency spectrum is increasing. Effort has been put into improving the coding, protocol and modulation of second generation systems while the role of the antenna has been largely overlooked [1]. Diversity schemes such as TDMA and CDMA are approaching their limitations [2]. Adaptive antennas may be used at the mobile base station to bring a considerable increase in channel capacity by using a frequency reuse method called space division multiple access (SDMA). The direction finding (DF) capability of adaptive antennas plays an important role in capacity enhancement. Therefore there is a significant need to develop high performance low cost DF systems. Direction finding systems need to perform well in complex signal environments in the presence of high powered co-channel interference. This requires expensive sophisticated equipment to sample the radio signal. DF has possibly remained primarily a military activity due to its high cost. Recently, various researchers [1, 3-6] have developed low cost direction finding systems based on mutual coupling with parasitic elements.

This paper aims to provide an insight into various low cost direction finding possibilities. While the topic of direction finding is widespread, the focus here is on low cost methods. The proposed methods will be simulated in SuperNEC [7] and Matlab. Thereafter, performance evaluations and comparisons between conventional and low cost techniques will be made.

In Section II various applications for direction finding are presented. Parasitic antennas and their use in DF are introduced in Section III. Section IV describes the configuration of the ESPAR antenna while the Reactance Domain MUSIC

algorithm is outlined in Section V. Simulations for all design parameters are shown in Section VI. A model was built and tested for verification purposes and the results are discussed in Section VII. The ESPAR is compared to conventional methods in Section VIII. Section IX presents the conclusions.

## II. APPLICATIONS OF DIRECTION FINDING

Direction finding has uses in a variety of applications. Traditionally, DF has been used mainly in military, defence, and law enforcement, but recently has found widespread application in consumer services especially in mobile phone location services. Table I presents common examples of these applications. Two of the current most important consumer applications are in GSM mobile phone location services and channel capacity improvement with SDMA. Ad-hoc networks and digital beamforming rely on DF principles to suppress interference and increase network throughput [8].

TABLE I DIRECTION FINDING APPLICATIONS

| Civil               | Military           | Commercial          | Research             |
|---------------------|--------------------|---------------------|----------------------|
| Travel information  | Monitoring enemies | Roadside assistance | Radio astronomy      |
| Search & rescue     | Electronic warfare | Theft recovery      | Earth remote sensing |
| Spectrum monitoring | Security           | Fleet management    | Corona detection     |
| Ad-Hoc networking   | Fighting crime     | Navigation          | Lightning detection  |

Mobile phone network DF applications incorporate those useful to network operators and consumers alike. Network operator services include the ability to monitor, in real time, the user distribution in a particular cell [9]. This leads to better system planning and increased channel capacity when high volume areas are sectored off within the GSM cell.

US authorities have paid particular attention to GSM location services and, in 1996, together with the Federal Communications Commission (FCC), launched the Enhanced 911 (E-911) initiative. The E-911 specification requires that any user who places an emergency call to 911 Emergency Services using a commercial wireless communications system should be located within 80m by the end of 2005 [9].

## III. PARASITIC ANTENNA OVERVIEW

### A. Initial Work

The concept of reactively loading antenna elements originated from Harrington [10], who proposed a method for reactively loading antennas to control radiation characteristics. This concept was furthered by various researchers such as Preston *et al.* [4, 11], Schlub *et al.* [12] and Scott *et al.* [13]. High

resolution DF algorithms based on parasitic antennas were researched by Svantesson *et al.* [6] and Ohira *et al.* at ATR of Japan [14].

Parasitic arrays follow from the concept of the Yagi-Uda array which comprises a reflector, active element and directors to focus the radiation [6]. A parasitic antenna typically has loaded monopoles that are arranged in a circle with the centre element active. The monopoles are loaded with reactances (varactor diodes) or switches (PIN diodes). Parasitic antennas rely on mutual coupling and the ability to vary the load at the base of the elements dynamically. This gives the antenna adaptive characteristics and therefore the antenna has the ability to direct radiation maxima and minima.

### B. Advantages of Parasitic Antennas

Parasitic antennas offer an attractive solution to low cost direction finding. In general, for a parasitic antenna, only one element is connected to a receiver. This reduces the amount of costly hardware and power consumption. Complexity is also reduced when compared to a conventional adaptive antenna as there are no phase shifters for beamforming. Since the reactances are typically diodes the switching times and scan times are short and suitable for use in TDMA applications such as GSM. Where conventional arrays suffer the effects of mutual coupling, parasitic antennas require coupling and are therefore free from its negative effects. Uniform Linear Arrays (ULA) perform inconsistently over azimuth with better performance at broadside than endfire, while these antennas are circular in geometry and immune to this problem. Parasitic antennas are flexible and may be used in DF, ad hoc networks or beamforming.

### C. Configurations of the Parasitic Antenna

There are two types of parasitic antennas of interest in direction finding. They may be classified as either switched beam or adaptive beam [15]. Both types are capable of adjustable radiation but only adaptive antennas are able to perform peak or null steering. This is due to the ability of the loads on each of the elements to change dynamically. Variable reactance allows for analogue control of the radiation pattern and together with a beam forming algorithm, the antenna becomes adaptive due to its ability to form and steer radiation lobes and nulls.

Switched beam antenna types have a limited set of beam possibilities but are still capable of offering significant spatial diversity and are much simpler than adaptive beam. There are two further configurations of switched beam antennas [4]. The first configuration has a centre element connected to a receiver with parasitic elements being switched in and out to form different radiation patterns [6]. The second configuration requires that the active element is switched between parasites performing the same function [11]. The parasites act as reflectors when shorted to ground via pin diodes and when not shorted have little effect on antenna performance [3]. It is then possible to sample the received signal with various radiation patterns.

### D. Direction Finding Techniques for Parasitic Antennas

There are various methods used to determine DOA using parasitic antennas. These vary from crude methods that sim-

ply detect the presence of a signal to the nearest quadrant [11] to high resolution algorithms with sub-degree accuracy [14].

In [16] an omni directional pattern is used to detect whether or not there in fact is a signal to be found. The signal is then divided into a number of sectors, i.e. a number of  $n$  directional patterns. The signal can then be determined to the nearest  $360^\circ/n$  area. This method is limited as it always finds the largest amplitude signal. Svantesson [6] and Ohira [17] have presented parasitic antennas employing high resolution algorithms that have sub-degree accuracy. This gives parasitic antennas an advantage in having a simple and cost effective DF solution. The Electronically Steerable Passive Array Radiator (ESPAR) is one such antenna.

## IV. THE ESPAR ANTENNA

### A. Basic Configuration

The Electronically Steerable Passive Array Radiator or ESPAR antenna was developed by the Advanced Telecommunications Research (ATR) Institute in Ktoyo, Japan [2]. Research has been done on the ESPAR antenna's capabilities for beamforming, ad-hoc networks and low cost direction finding.

The antenna is a multi-element parasitic array with a single active element. In its typical design, the array has six reactively loaded monopoles arranged in a circle, with a centre monopole that is either active or fed to a receiver. All the elements in the array ideally rest on an infinite ground plane. The ESPAR antenna in its typical configuration is shown in fig. 1.

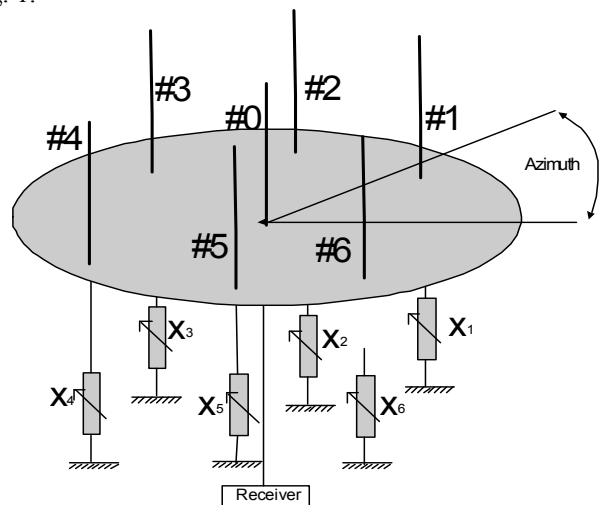


Fig. 1. The configuration of the ESPAR antenna

The antenna has the ability to change its radiation pattern by varying the reactive loads at the base of each monopole, which in turn, changes the current distribution on each element. Therefore the antenna has beamforming and adaptive capabilities. Capacitive varactor diodes have been suggested for the reactances together with RF chokes and DC control voltages [2].

The design parameters of the ESPAR are shown in Table II. The ESPAR antenna is synonymous with the work done by Harrington and Mautz [18] that developed the  $N$ -port network of a reactively loaded dipole array. The ESPAR requires monopoles placed on a ground plane where the ground plane serves to shield the reactance control circuitry physically and electrically.

TABLE II ESPAR DESIGN PARAMETERS

| Parameter              | Symbol            | Initial Value |
|------------------------|-------------------|---------------|
| Number of Elements     | $M$               | 6             |
| Element height         | $H_p$             | $0.25\lambda$ |
| ESPAR Diameter         | $D_e$             | $0.5\lambda$  |
| Load reactances        | $x_1, \dots, x_6$ |               |
| Ground plane Diameter  | $D_g$             | $1\lambda$    |
| Ground Skirting Height | $H_s$             | $0.25\lambda$ |

### B. Signal Model

This signal model is specific to the ESPAR antenna and a model suitable for the Reactance Domain multiple signal classification (MUSIC) algorithm is presented. The assumptions for this model are line of sight propagation with no multipath components.

The antenna in its basic form consist of  $M+1$  elements where  $M = 6$  in this configuration. The  $M$  elements are parasitic and arranged in a circle with the  $0^{\text{th}}$  active element at the centre of the ground plane. The pattern of the antenna is controlled by the reactances  $x_m$  ( $m = 1, 2, \dots, M$ ) which are placed at the bottom of the  $M$  elements. The reactance vector is denoted as

$$\mathbf{x} = [x_1, x_2, \dots, x_M]^T \quad (1)$$

where the superscript  $T$  denotes the transpose operation.

Assume that there are  $D$  transmitted signals  $u_d(t)$  with DOAs  $\theta_d$  ( $d = 1, 2, \dots, D$ ). Let  $s_m(t)$  denote the signal received at the  $m^{\text{th}}$  element of the antenna and let  $\mathbf{s}(t)$  be the column vector with  $m^{\text{th}}$  component  $s_m(t)$ . Therefore the column vector  $\mathbf{s}(t)$  can be expressed as

$$\mathbf{s}(t) = \sum_{d=1}^D \mathbf{a}(\theta_d) u_d(t) \quad (2)$$

where  $\mathbf{a}(\theta_d)$  is the steering vector of the ESPAR and depending on its configuration can be expressed as

$$\mathbf{a}(\theta_d) = \left[ 1, e^{j\frac{\pi}{2}\cos(\theta_d - \varphi_1)}, \dots, e^{j\frac{\pi}{2}\cos(\theta_d - \varphi_M)} \right]^T \quad (3)$$

where  $\varphi_m = (2\pi / M)(m - 1)$  ( $m = 1 \dots M$ ) corresponds to the  $m^{\text{th}}$  element position relative to an arbitrary axis.

The output of the ESPAR antenna can be given as

$$\mathbf{y}(t) = \sum_{d=1}^D \mathbf{i}^T \mathbf{a}(\theta_d) u_d(t) + n(t) = \mathbf{i}^T \mathbf{s}(t) + n(t) \quad (4)$$

where  $n(t)$  is assumed to be additive white Gaussian noise and  $\mathbf{i}$  is the RF current vector. The  $\mathbf{i}$  vector can be formulated as

$$\mathbf{i} = \mathbf{V}_s (\mathbf{Z} + \mathbf{X})^{-1} \mathbf{u}_0 \quad (5)$$

where the matrix  $\mathbf{X} = \text{diag}[50, jx_1, jx_2, \dots, jx_M]$  is a diagonal matrix termed the reactance matrix and  $\mathbf{u}_0 = [1, 0, \dots, 0]^T$  is  $(M+1)$  dimensional [19]. The  $\mathbf{Z}$  matrix is square and of dimension  $(M+1)$  and is determined by the mutual impedance between the elements.  $\mathbf{V}_s$  is a constant and taken to be the source voltage of the active RF radiator. The current vector  $\mathbf{i}$ , and therefore the output  $\mathbf{y}(t)$ , is a function of  $\mathbf{x}$ .

It is assumed that (4) refers to an antenna in transmit mode. The theorem of reciprocity holds that the radiation pattern of the antenna in transmit and receive mode will be identical. In receive mode the  $\mathbf{i}$  vector should be seen as a weight vector

since it acts like a weight in a conventional adaptive array antenna [14].

## V. REACTANCE DOMAIN MUSIC ALGORITHM

Previous methods for DF with parasitic antennas used switched beams such as the one documented by Gyoda and Ohira in [5]. In this technique twelve beams are switched to find the directions of the signals, but the resolution is limited to  $30^\circ$  and precision to only  $15^\circ$ . The following adaptation of the popular MUSIC algorithm [20] offers a solution with significant improvement.

### A. Single-Port Correlation Matrix

The conventional MUSIC algorithm [20] requires that a correlation matrix be estimated from the array sensors. Since the signals on each of the elements cannot be observed at the same time, the signal must be retransmitted and measured  $M$  times [14]. By repeating the signal  $M$  times, the  $M$  output values are obtained as if an  $M$  element antenna had been used. Each time the signal is transmitted a different set of reactances is used. This is shown in fig. 2. The spatial diversity of a conventional array is recreated in this way. From this it is clear that the ESPAR can only be used with periodic signals [17]. Now the correlation matrix can be created using conventional techniques.

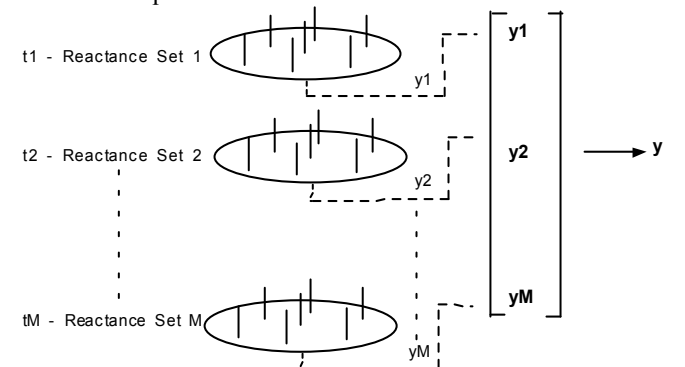


Fig. 2. The formation of the correlation matrix in Reactance Domain MUSIC

### B. Reactance Domain MUSIC

The received signal at the centre element of the ESPAR antenna is a combination of wave fronts and noise. The output of the ESPAR antenna, according to (5) is computed by finding the current vector  $\mathbf{i}$  for a given set of reactances [17]. The  $\mathbf{y}$  output vector can then be used to compute the correlation matrix.

The  $M$  outputs of the antenna can be expressed as

$$y_m(t_m) = \sum_{d=1}^D \mathbf{i}_m^T \mathbf{a}(\theta_d) u_d(t_m) + n(t_m) \quad (6)$$

under the assumption that

$$u_d(t_1) = u_d(t_2) = \dots = u_d(t_M) \quad (7)$$

for  $d=1, \dots, D$ . This implies that the MUSIC algorithm requires that the signal remain constant over the  $M$  sampling periods.

The output vector  $\mathbf{y}$  can be denoted as (time index omitted)

$$\mathbf{y} = \mathbf{I}^T \mathbf{A} \mathbf{u} + \mathbf{n} \quad (8)$$

The modified steering vector can be expressed as

$$\mathbf{a}_{\text{mod}}(\theta) = \mathbf{I}^T \mathbf{a}(\theta) \quad (9)$$

The correlation matrix of the ESPAR antenna is therefore

$$\mathbf{R}_{yy} = \mathbf{E}[\mathbf{y}\mathbf{y}^H] \quad (10)$$

The Reactance MUSIC spectrum then becomes [20]

$$P_{\text{MU}}^{\text{ESPAR}}(\theta) = \frac{1}{\mathbf{a}_{\text{mod}}(\theta)^H \mathbf{E}_N \mathbf{E}_N^H \mathbf{a}_{\text{mod}}(\theta)} \quad (11)$$

for  $0^\circ < \theta < 360^\circ$ , where  $^H$  denotes Hermitian transpose.  $\mathbf{E}_N$  is defined to be the matrix of noise Eigenvectors of dimension  $M$  by  $(M - D)$ . The DOA can now be evaluated by finding peaks of the MUSIC spectra.

## VI. ESPAR SIMULATIONS

The design of an ESPAR antenna relies on various parameters and the affect of each of these parameters on the DF performance was analysed in SuperNEC. Schlub [2] tested three packages for suitability for simulating the ESPAR antenna (NEC, HFSS v7.0 and XFDTD v5.1) and showed that NEC was adequate in accuracy but considerably faster in simulation time. SuperNEC is a MoM/UTD program based on NEC2 [7] and was used for all simulations. The DF signal processing algorithms were calculated in Matlab. SuperNEC proved to be ideal for this study due to its ability to be called in batch mode and analyse large samples of data.

For generality all dimensions will be quoted in terms of wavelengths. Antennas are modelled in the receiving case and the sources are in the far field of the receiver antenna. Doppler frequency shift is ignored in all cases.

### A. Number of Parasitic Elements

In previous papers by Ohira *et al.*, the number of parasitic elements is 6 [14]. This affects the dimension of the correlation matrix for the Reactance MUSIC algorithm. Therefore the estimation time would be less for fewer elements as the signal would need to be retransmitted less times. The number of elements also controls the radiation pattern, which is responsible for recreating the spatial diversity. If the number of elements is too low it is not possible to create a radiation pattern with a shape suitable for the Reactance MUSIC to estimate the DOA correctly. The cost of conventional arrays increase dramatically if an element is added as an extra receiver is also required. In the ESPAR configuration adding an element does not require a new receiver but only reactance control circuitry. Therefore adding an element does not significantly increase the cost of the system.

Simulations were therefore done to investigate the performance for various numbers of elements. SuperNEC results show that the best number of elements remains at 6 [21]. A fewer number of elements requires a higher signal-to-noise-ratio (SNR) for good performance. A 6 element antenna at 20dB SNR performs equally to a 3 element at 35dB SNR [21]. The number of resolvable signals is still  $M-1$ , which is the same for conventional arrays. In general, the more elements there are the deeper and sharper the MUSIC spectrum peaks are. However, the more elements there are the more complex it is to find a set of workable reactances. Since the reactance set was chosen randomly there exists a possibility for superior performance with more or less elements.

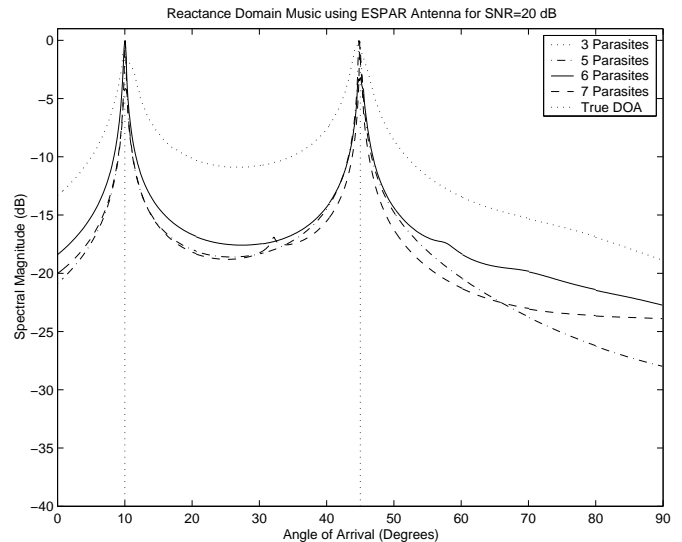


Fig. 3. MUSIC spectra for ESPAR antennas of different number of elements

### B. ESPAR Diameter

The diameter of the ESPAR is specified at  $0.5\lambda$  [14]. Simulations were done with various diameters to determine the DOA performance, impedance and radiation pattern [21] variation with diameter. All parameters were kept constant in the simulations, while only the diameter was varied from  $0.25\lambda$  to  $1\lambda$ . The simulations show that the radiation pattern, impedance and DF performance are affected by the diameter. This proves that the ESPAR relies on mutual coupling. Radiation patterns for various diameters are shown in fig. 4.

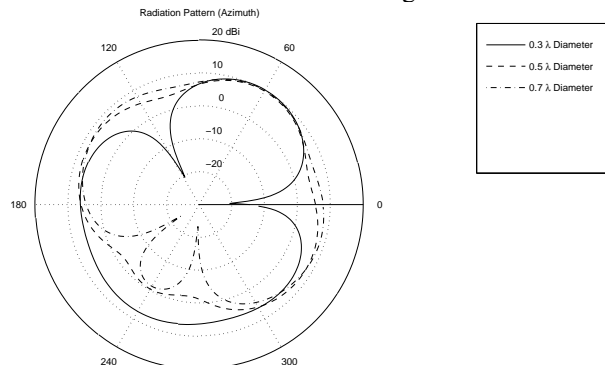


Fig. 4. Radiation patterns for ESPAR of various diameters

The radiation pattern shows deep nulls above and below  $0.5\lambda$  diameter, making  $0.5\lambda$  ideal. This explains why the DOA performance is good for diameters below  $0.5\lambda$  while it drops above  $0.5\lambda$ . The Smith chart in fig. 5 shows that reactance increases with diameter.

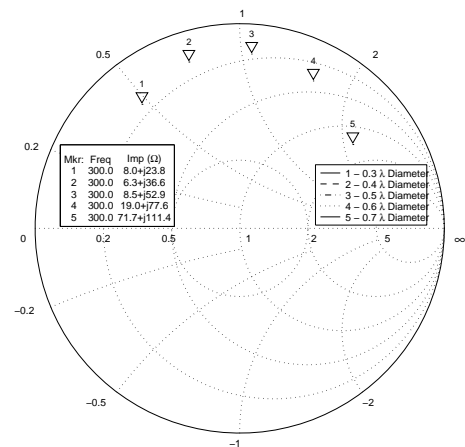


Fig. 5. Smith chart of impedance for increasing ESPAR diameter

### C. Performance of the Reactance Domain MUSIC Algorithm

#### 1) Snapshots

The importance of the number of snapshots used to estimate the signal correlation matrix has been investigated and shown in fig. 6.

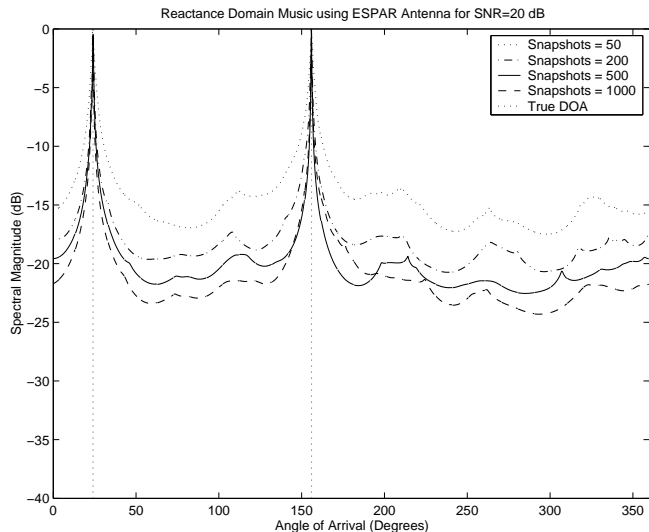


Fig. 6. Reactance MUSIC spectra for various numbers of snapshots

From fig. 6 it can be seen that the algorithm produces sharper peaks in the Reactance MUSIC spectra when more snapshots are used, but even when 50 snapshots are used the DOA resolution is still good [21]. In this case the SNR is 20dB. The computational burden is lower for fewer snapshots and hence it is faster to estimate a correlation matrix with 50 snapshots than it is for 500 snapshots.

#### 2) Additive Noise

Additive noise with a white Gaussian distribution having unity variance and zero mean was added to corrupt the signal data [21]. The noise was uncorrelated with the desired signals. It can be seen from fig. 7 that a higher SNR produces sharper peaks and so resolution and precision increase with SNR [17].

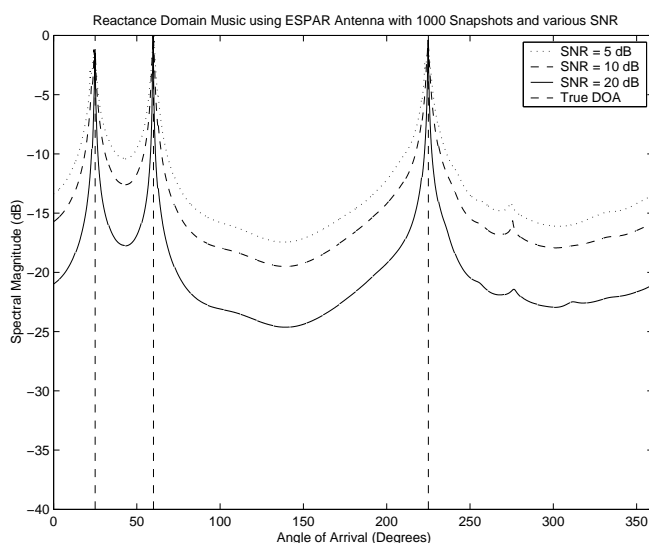


Fig. 7. Reactance Music spectra for various signal-to-noise ratios

When the SNR is low, the noise corrupts the signal data heavily and this results in spurious peaks in the output spectra that may be misleading. A statistical analysis was therefore done to test the ESPAR over a large sample and is discussed later.

#### 3) Number of Resolvable Signals

The number of resolvable signals from Reactance MUSIC is limited by the number of parasitic elements. This limits the dimension of the correlation matrix. The number of resolvable signals is therefore limited to  $M-1$  and is identical to the case for a conventional ULA with regular MUSIC algorithm.

#### 4) Periodicity of Incoming Signals

Sun and Karmakar [1] performed tests where a desired signal was repeated periodically, while interference was intermittent. The result shows that Reactance MUSIC cannot estimate the direction of the interferences in this case but the desired signal's DOA can be found easily. This shows that provided a signal has a periodic property it can be resolved.

#### 5) Signal Separation

Signals as close as  $0.2^\circ$  could be distinctly determined when the SNR was above 55dB [21]. Should two signals approach from the exact same direction only one peak will be seen in the spectra and it may not be possible to determine that there are two signals. Fig. 8 shows the relationship between angular resolution and SNR for the 6 element ESPAR.

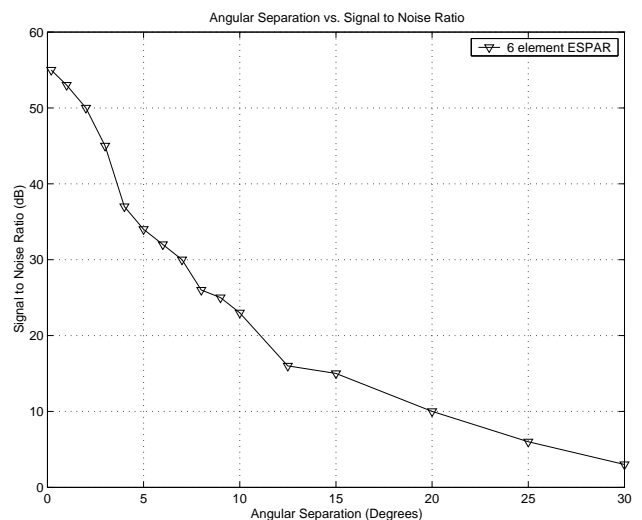


Fig. 8 Angular resolution limits for various signal-to-noise ratios

#### 6) Signals having different Power Levels

It is likely that desired signals will impinge on the ESPAR with different power levels. Reactance MUSIC is capable of resolving signals with different powers provided that the lowest power signal has at least 25% of full power [21].

#### 7) Load Reactances

The load reactances at the bases of the parasitic elements are critical components in the ESPAR antenna. These reactances are responsible for forming the radiation pattern, which is used to recreate spatial diversity to determine the DOA of signals. The radiation pattern should be asymmetrical and non-uniform as required by the MUSIC algorithm. The radiation pattern should not be confused with one used for beam-forming where a narrow, high gain peak is ideal. A pattern with peaks and deep nulls is not suitable either as the desired signal would be undetectable [1].

Simulations were done to determine the affect of various combinations of loads on the MUSIC algorithm and to determine which set is ideal. It is important to appreciate that the ESPAR has a complex structure and hence there is a need to optimise for both reactance and physical make up [2]. It would be impossible to test every combination of load reac-

tances and physical parameters so a sample set of potentially useful reactances was selected for further analysis.

The fifteen sets of reactances that were selected for further analysis are shown in Table III with their results.

TABLE III ESPAR LOAD REACTANCES

| Set No. | Load Type    | DOA | Radiation Pattern |
|---------|--------------|-----|-------------------|
| 1       | Zero         | No  | Uniform           |
| 2       | Equal        | No  | Uniform           |
| 3       | Ordered      | No  | Uniform           |
| 4       | Capacitive   | Yes | Asymmetrical      |
| 5       | Inductive    | Yes | Asymmetrical      |
| 6       | Max/Min/Zero | Yes | Asymmetrical      |
| 7       | Optimised    | Yes | Asymmetrical      |
| 8       | Real only    | Yes | Asymmetrical      |
| 9       | Limited 25   | Yes | Asymmetrical      |
| 10      | Random1      | Yes | Asymmetrical      |
| 11      | Random2      | Yes | Asymmetrical      |
| 12      | Random3      | Yes | Asymmetrical      |
| 13      | Random4      | Yes | Asymmetrical      |
| 14      | Random5      | Yes | Asymmetrical      |
| 15      | Random6      | Yes | Asymmetrical      |

In all cases except the Limited 25 set, the reactances were limited to the range  $\pm 100j$ . From the table it is clear that DOA cannot be resolved when equal or ordered loads are used [21]. This is due to a uniform radiation pattern. A symmetrical pattern cannot be virtually rotated and affords no spatial diversity. All other reactance sets are capable of resolving the DOA due to their non-uniform radiation patterns. Some combinations of reactances produce deeper nulls than others. Radiation patterns are shown in fig. 9.

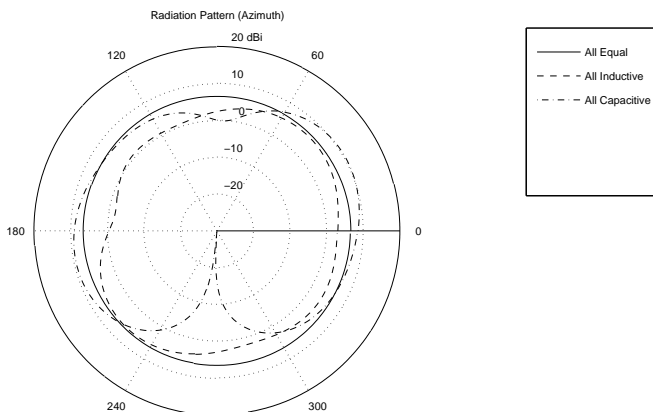


Fig. 9. Radiation pattern for various load combinations

### 8) Azimuth & Elevation Coverage

The ESPAR antenna is capable of resolving signals over the full azimuth equally well [21]. This is in contrast to the performance of the ULA which only performs over  $180^\circ$  without ambiguity errors and performs better at broadside than end-fire. All that is required is an asymmetrical radiation pattern.

The results from simulations for elevation coverage are surprising. The ESPAR is capable of detecting a signal from an elevation of  $20^\circ$ . The peak in the spectra is far lower than the corresponding peak from a  $90^\circ$  elevation. Because the peak is so small it might be confused with a spurious peak caused by noise and the signal can be missed. Elevation angles above

$45^\circ$  produce a detectable peak. Various elevation angles in the MUSIC spectra are shown in fig. 10.

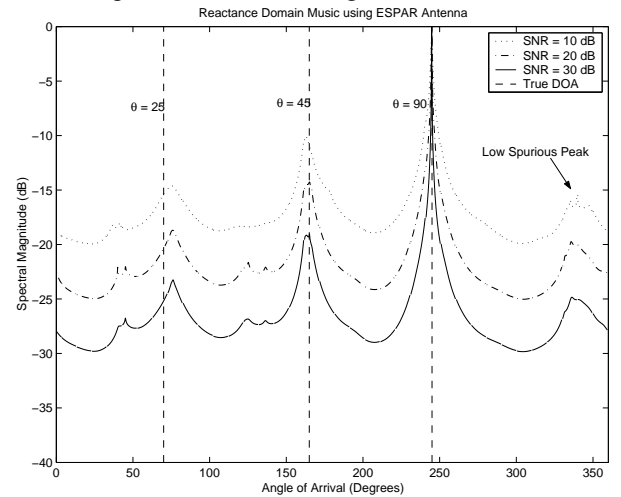


Fig. 10. Reactance MUSIC spectra for various elevation angles

### 9) Frequency Response

Since the reactances are frequency dependant, it is necessary to explore what useful bandwidth the ESPAR has for various reactance sets. Ito *et al.* [22] shows ESPAR gain-bandwidth to be 15% or more using a Monte Carlo method for a dynamic reactance range of  $-j100 \Omega < X_m < j100 \Omega$ . Bandwidth drops by half if the reactance only takes positive values.

Simulations show that it is difficult to yield an impedance bandwidth with a VSWR below 5:1 of more than 10% [21]. As the frequency moves away from the design centre frequency, the MUSIC spectra peaks get shallower. Some reactance sets perform significantly better than others and a more advanced technique is required to solve this problem. In various applications a wide bandwidth antenna or dual frequency antenna is required. The ESPAR at this stage is not capable of sustaining a wide bandwidth or dual-band operation due to the frequency sensitivity of its complex construction.

### 10) Speed of DOA Estimation

If the ESPAR is to be used in communication systems and especially TDMA systems it must have a fast DOA acquisition time. In GSM, a time slot is only  $577\mu s$  long so the ESPAR needs to be able to reconfigure the reactances 6 times and make measurements in this short time. If varactor diodes are used, the tuning of reactances should be able to be done in a few nanoseconds and therefore this system should be suitable for GSM and other TDMA systems.

### 11) Performance in a Correlated Noise Environment

For the ESPAR DF system to be useful in a communications system, it must be capable of working in a multipath signal environment. Hirata *et al.* [23] has shown that the ESPAR is capable of resolving the DOA of coherent signals using a variation of the Reactance MUSIC algorithm. Spatial Smoothing Pre-processing (SSP) has the ability to suppress coherence between waves by dividing arrays into parallel overlapping sub arrays for DOA estimation. The proposed method divides the ESPAR into three parallel overlapping diamond-shaped sub-arrays. Three pairs of diamond sub-arrays are formed with the six parasitic elements. A combination of three MUSIC spectra on each pair of diamond shaped sub arrays reduces the limitation of coherent waves and DOA estimation. SSP is performed by computing  $\mathbf{R}_{yy}$  the normal

way and a correlation matrix  $\mathbf{R}_b$  is then formed by forward-backward averaging. This technique fails for the case of two sources at  $90^\circ$  and  $270^\circ$  which is due to the fact that phase information cannot be extracted from these directions. However, using the proposed procedure it is possible to separate two coherent signals without dependence on the DOA's.

#### D. Statistical Analysis

In the previous simulations, noise was added to corrupt the signals. It was shown that in some cases spurious peaks in the spectra were obtained, especially for low SNR. This is due to the randomness of the added noise. Fig. 11 shows 250 cases of MUSIC spectra at 20dB each with different noise added.

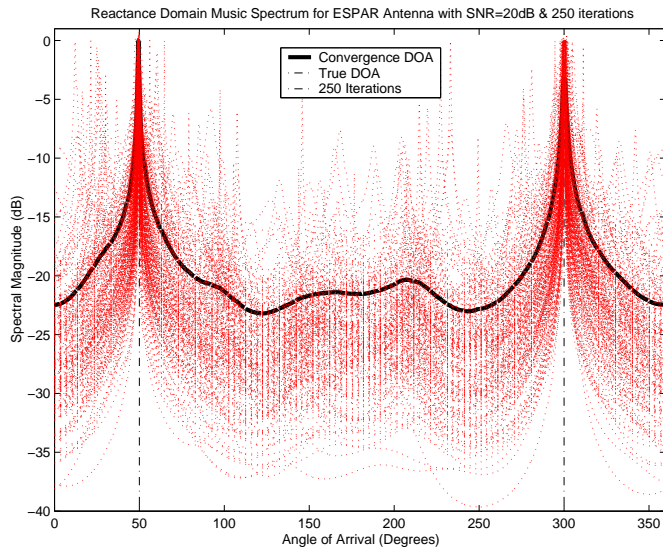


Fig. 11. Statistical analysis of Reactance MUSIC spectra for 250 trials

Matlab was used to estimate thousands of Reactance MUSIC spectra, each time using a new state of the random number generator [21]. Fig. 11 demonstrates that the algorithm will converge to the correct DOA for any number of trials.

### VII. CONSTRUCTION & TESTING

A proof of concept model was constructed for verification purposes. The model consisted of two monopoles on an electrically large ground plane, where the centre element was connected to a vector network analyser and the second parasitic element was loaded with various reactances. Varactor diodes and static impedances were used for the reactances. All measurements were made in an anechoic chamber with no obstructions at 300 Mhz. The monopoles were  $0.25\lambda$  in height with a spacing of  $0.25\lambda$ .

The results showed that by changing the impedance at the base of a monopole, the radiation pattern and input impedance to the centre element can be controlled. This result agrees with the SuperNEC simulations and therefore it can be deduced that by varying the impedances of six elements surrounding an active monopole, the radiation pattern and input impedance can be controlled.

### VIII. PERFORMANCE COMPARISON TO EXPENSIVE METHODS

Investigations were done to compare the performance of a 6 element ULA and a 6 element ESPAR [24]. The results of the comparison are shown in Table IV.

TABLE IV COMPARISON OF THE ESPAR TO THE ULA

| Parameter                       | ULA                      | ESPAR  |
|---------------------------------|--------------------------|--|
| Number of Signals               | 5 ( $M-1$ )              | 5 ( $M-1$ )                                  |
| Azimuth (Deg.)                  | $180^\circ$              | $360^\circ$                                  |
| Elevation (Deg.)                | Limited – spurious peaks | Limited to 20 degrees – Good from $45^\circ$ |
| Signal Separation @ 40dB (Deg.) | $2^\circ$                | $2.5^\circ$                                  |
| Ground Plane                    | No                       | Required                                     |
| Periodic Signals                | Any type                 | Required                                     |
| Cost                            | $M$ cost units           | 1 cost unit                                  |
| Complexity                      | Complex                  | Simpler                                      |
| DOA Acquisition Time            | 1 time step              | $M$ time steps                               |

The performance of the antennas is similar showing that the ESPAR does compete on performance. However, the limitations of the ESPAR can be summarised as follows. Only periodic signals can be resolved and the acquisition time is therefore  $M$  times longer as the signal is resent  $M$  times. The ESPAR requires a ground plane which is of finite size. This causes an offset in the elevation radiation pattern and may result in degraded radio links. A ULA is simple to construct and install while the ESPAR's biggest challenge is getting repeatable consistent performance from varactor diodes.

However, since the ESPAR is circular it is capable of resolving signals equally well over full azimuth. A ULA is limited to  $180^\circ$  coverage and suffers ambiguity errors. A ULA also typically performs better at broadside and worse at end fire. The ESPAR's reduction in performance is minimal compared to the large cost saving provided.

### IX. CONCLUSIONS

The ESPAR antenna developed by ATR in Japan was analysed to determine its feasibility in low cost DF applications. The antenna was simulated in SuperNEC and the Reactance MUSIC algorithm was used to establish the DOA information.

The simulation results showed that the optimum number of elements is 6 with an array diameter of  $0.5\lambda$ . This agrees with the findings of ATR. The Reactance Domain MUSIC algorithm performed well showing comparative results with the conventional MUSIC algorithm. The number of resolvable signals is 5 ( $M-1$ ) while signals as close as  $0.2^\circ$  at SNR of 55dB can be determined. For low SNR and fewer elements, maxima in the MUSIC spectra are shallow making it difficult to determine true signals from spurious peaks. Signals having 25% of full power produce detectable peaks and elevation angles above  $45^\circ$  are resolvable. The load reactances at the bases of the parasites control the radiation pattern of the array. For the DOA to be resolved the pattern should be asymmetrical. Randomly selecting reactances produces good resolution but it is difficult to yield an impedance bandwidth with a VSWR below 5:1 of more than 10%. This indicates that a more advanced method of selecting reactance sets is required.

The simulation results show that the ESPAR does offer excellent overall performance despite the reduction in cost. In



comparison to the conventional ULA, the ESPAR performs well. Further work is required to optimise the reactances for wide bandwidth operation and determine the capability for mass production and reliable reactance control.

#### X. REFERENCES

- [1] C. Sun, N. Karmakar, "Direction of Arrival Estimation with a novel single-port smart antenna.", *EURASIP Journal on App. Sig. Processing*, vol. 2004:9, 1364-1375.
- [2] R.W. Schlub, "Practical Realization of Switched and Adaptive Parasitic Monopole Radiating Structures.", PhD dissertation, School of Microelectronic Engineering, Griffith University, January 2004.
- [3] T. Svantesson, M. Wennstrom, "An Antenna Solution for MIMO Channels: The Switched Parasitic Antenna.", *IEEE Symposium on Personal Indoor and Mobile Radio Communication (PIMRC) 2001*, San Diego, USA, September 30 - October 3 2001.
- [4] S.L. Preston, D.V. Thiel, J.W. Lu, S.G. O'Keefe, T.S. Bird, "Electronic beam steering using switched parasitic patch elements", *Electron. Lett.*, 1997, vol. 33, no.1, pp. 7-8.
- [5] T. Ohira, K. Gyoda, "Hand-held microwave direction-of-arrival finder based on varactor-tuned analog aerial beamforming", *Proc. Asia-Pacific Microwave Conference*, Taipei, Dec. 2001, pp.585-588.
- [6] T. Svantesson, M. Wennstrom, "High resolution direction finding using a switched parasitic antenna.", *Proc. 11<sup>th</sup> IEEE Signal Processing Workshop on Statistical Signal Processing*, Singapore, Aug. 2001, pp. 508-511.
- [7] D. C. Nitch, "A serial and parallel design of NEC2 to demonstrate the advantages of the object-oriented paradigm in comparison with the procedural paradigm". Phd thesis, School of Electrical Engineering, University of the Witwatersrand, December 1992.
- [8] C. Sun, A. Hirata, T. Ohira, N. Karmakar, "Fast Beamforming of Electronically Steerable Parasitic Array Radiator Antennas: Theory and Experiment", *IEEE Trans. Antennas Propagat.*, vol. 52, no. 7, July 2004.
- [9] C.W. Kain, "Location-Based Wireless Services: Finding People Everywhere", Chapter 3, pp. 19-24. <http://www.mitrek.org/home.nsf/Publications/SigmaSpring2002>
- [10] R.F. Harrington, "Reactively controlled directive arrays", *IEEE Trans. on Antennas Propagat.*, vol AP-26, pp. 390-395, May 1978.
- [11] S.T. Preston, D.V. Thiel, T.A. Smith, S.G. O'Keefe, J.W. Lu "Base-station tracking in mobile in mobile communications using a switched parasitic antenna array", *IEEE Trans. Antennas Propagat.*, vol. AP46, pp. 841-844, Jun. 1998.
- [12] R. Schlub, D.V. Thiel, J.W. Lu, S.G. O'Keefe, "Dual-band six-element switched parasitic array for smart antenna cellular communications systems.", *Electron. Lett.*, 2000, vol. 36, no. 16, pp. 1342-1343.
- [13] N.L. Scott, M.O Leonard-Taylor, R.G. Vaughan, "Diversity Gain from a single port adaptive antenna using switched parasitic elements illustrated with a wire and monopole prototype.", *IEEE Trans. Antennas Propagat.*, vol. 47, no. 6, pp.1066-1070, Jun. 1999.
- [14] Plapous, P., Cheng, J., Taillefer, E., Hirata, A., Ohira, T., "Reactance Domain MUSIC Algorithm for Electronically Steerable Parasitic Array Radiator", *IEEE Trans. Antennas Propagat.*, vol. 52, No. 12, pp. 3257-3263, December 2004.
- [15] M. Chryssomallis, "Smart Antennas", *IEEE. Trans. Antennas Propagat. Magazine*, vol. 42, pp.129-136, June 2000.
- [16] A. Kallis, T. Antonakopoulos, "Direction Finding in IEEE802.11 Wireless Networks", *IEEE Trans. Measu. Instr.*, vol. 51, no. 5, pp. 940-948, October 2002.
- [17] C. Plapous, J. Cheng, E. Taillefer, A. Hirata, and T. Ohira, "Reactance domain MUSIC algorithm for ESPAR antennas," in *Proc. 33rd European Microwave Conference*, vol. 2, 2003, pp. 793-796.
- [18] J.R. Mautz, R.F Harrington, "Control of Radar scattering by reactive loading.", *IEEE Trans. Antennas Propagat.*, vol. AP-20, pp.446-454, July 1972.
- [19] J. Cheng, Y. Kamiya, and T. Ohira, "Adaptive beamforming of ESPAR antenna based on steepest gradient algorithm", *IEICE Trans. Commun.*, vol. E84-B, pp. 1790-1800, July 2001.
- [20] R. O. Schmidt, "Multiple emitter location and signal parameter estimation", *IEEE Trans. Antennas and Propagat.*, vol AP-34, pp. 276-280, March 1986.
- [21] J.M. Berger, "Low Cost Direction Finding with the Electrically Steerable Parasitic Array Radiator (ESPAR) Antenna", MSc. Dissertation, School of Electrical & Information Engineering, University of the Witwatersrand, 2005, Appendix A: ESPAR Antenna Simulation Results
- [22] K. Ito, A. Akiyama, M. Ando, "Bandwidth of Electronically Steerable Parasitic Array Radiator in Single Beam Scanning", *IEICE Trans Commun.*, vol. 86-B, no.9, September 2003.
- [23] A.Hirata, T. Aono, H. Yamada, and T. Ohira, "Reactance-Domain SSP MUSIC for an ESPAR antenna for estimate the DOAs of coherent waves," in *Proc. Int. Symposium on Wireless Personal Multimedia Communications*, Yokohama, 2003, pp. 242-246.
- [24] J.M. Berger, "Low Cost Direction Finding with the Electrically Steerable Parasitic Array Radiator (ESPAR) Antenna", MSc. Dissertation, School of Electrical & Information Engineering, University of the Witwatersrand, 2005, Appendix B: Uniform Linear Array and ESPAR Performance Comparison Simulations

# Appendix A: ESPAR Antenna Simulation Results

## Abstract

Simulations to investigate the performance of ESPAR antenna are presented. The Reactance domain MUSIC algorithm was used to determine the direction of arrival information. The results show that the ESPAR performs best with 6 parasitic elements arranged in a circle of diameter  $0.5\lambda$ . The algorithm performs better with more snapshots, but is capable of resolving signals with only 50 snapshots. Spurious peaks in the MUSIC spectra are caused by signal to noise ratios (SNR) below 10dB. Azimuth separations of  $0.2^\circ$  are resolved when SNR is above 55dB but lower SNR produces good results for wider angular separations.. Elevations as steep as  $45^\circ$  produce detectable peaks in the spectrum and hence can be resolved. Various power level signals can be determined as low as 25% of full power. A random set of reactances will, in general, be able to determine the direction of arrival but the VSWR performance will not be below 5:1 for more than 10 % bandwidth. An in depth optimization scheme such as a genetic algorithm is required to determine the best set of reactances based on DOA performance and VSWR.

## A. Introduction

The simulation results used to investigate the performance of the Electronically Steerable Parasitic Array Radiator (ESPAR) antenna are presented. All simulations were done with SuperNEC and hence an infinite ground plane is assumed. In the interest of generality the simulation frequency was 300 MHz so all resulting parameters are expressed in terms of wavelength. Unless otherwise specified the elevation angle is constant at  $90^\circ$ .

## B. The SuperNEC Model

SuperNEC was used in all simulations to model the performance of the ESPAR antenna. The model consists of 6 reactively loaded monopoles on an infinite ground plane. The centre monopole is loaded with  $50\ \Omega$  and the currents on the load segment are analysed and used in the Reactance Domain MUSIC algorithm.

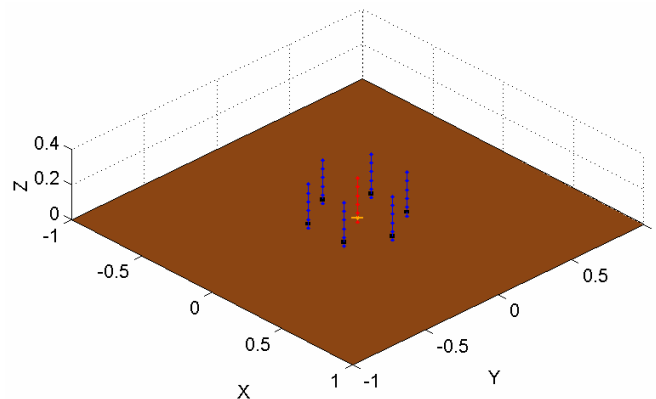


Fig. 12 The SuperNEC model of the ESPAR antenna

## C. Number of Elements

Simulations to predict the performance of the ESPAR for various numbers of parasitic elements were performed. The goal was to determine what the best configuration is for this antenna. Simulations were done for the following combinations:

- 3 Elements
- 5 Elements
- 6 Elements
- 7 Elements

In all cases of the simulations the simulation frequency, load reactances, antenna diameter are kept constant. The azimuth angle range covers 0 to 90 degrees.

1) 3 Element ESPAR Antenna

The results for Reactance Music algorithm are presented for an ESPAR antenna with 3 elements. The reactances used in this case were:  $X_1 = 0 -14i$ ,  $X_2 = 0 -65i$  and  $X_3 = 0 +39i$ .

The 3 element cannot resolve more than 2 signals and it demands a high SNR to be able to resolve signals accurately. Fig. 13 shows that peaks are created in the spectrum but they are not deep and sharp.

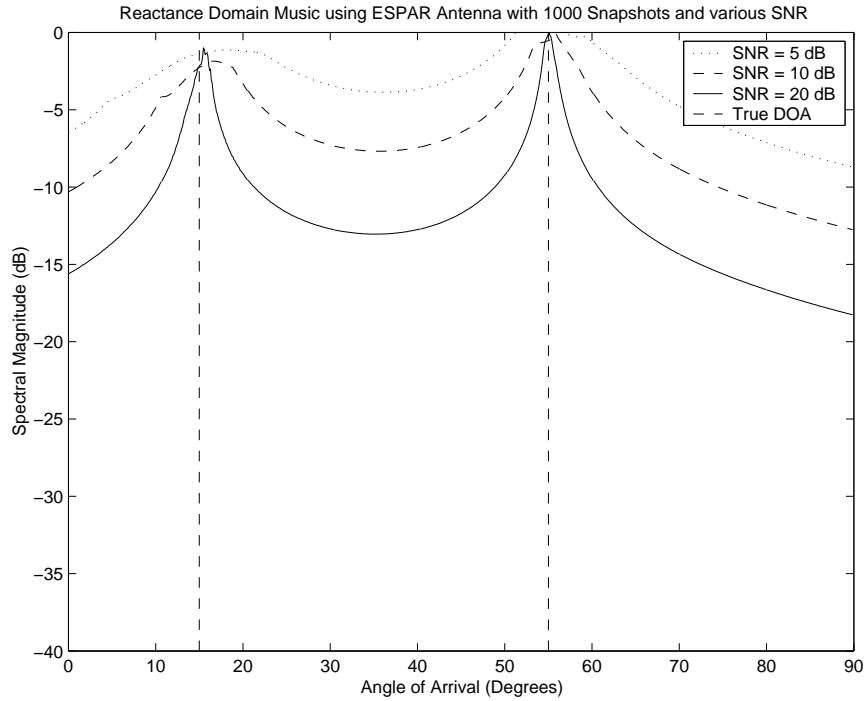


Fig. 13 Reactance MUSIC spectra for various signal-to-noise ratios for the three element ESPAR

2) 5 Element ESPAR Antenna

The results for Reactance Music algorithm are presented for an ESPAR antenna with 5 elements. The reactances used in this case were:  $X_1 = 0 -14i$ ,  $X_2 = 0 -65i$ ,  $X_3 = 0 +39i$ ,  $X_4 = 0 +17i$  and  $X_5 = 0 +39i$ .

The 5 element cannot resolve more than 4 signals and it performs well even in moderate SNR environments.

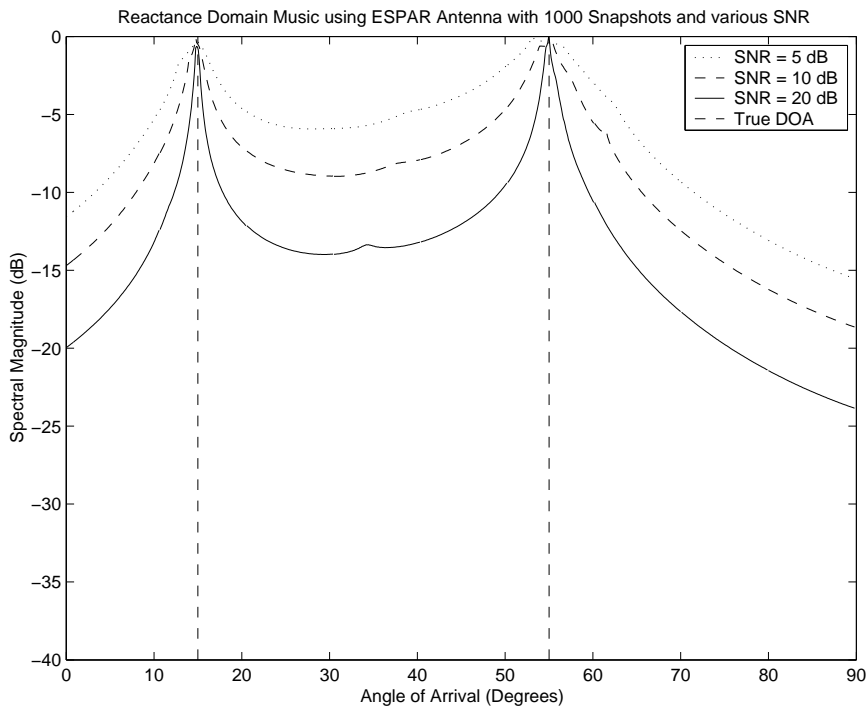


Fig. 14 Reactance MUSIC spectra for various signal-to-noise ratios for the five element ESPAR

3) 6 Element ESPAR Antenna

The results for Reactance Music algorithm are presented for an ESPAR antenna with 5 elements. The reactances used in this case were:  $X_1 = 0 -14i$ ,  $X_2 = 0 -65i$ ,  $X_3 = 0 + 39i$ ,  $X_4 = 0 +17i$ ,  $X_5 = 0 +39i$  and  $X_6 = 0 -65i$ .

The 6 element cannot resolve more than 5 signals and it performs well even in all SNR environments.

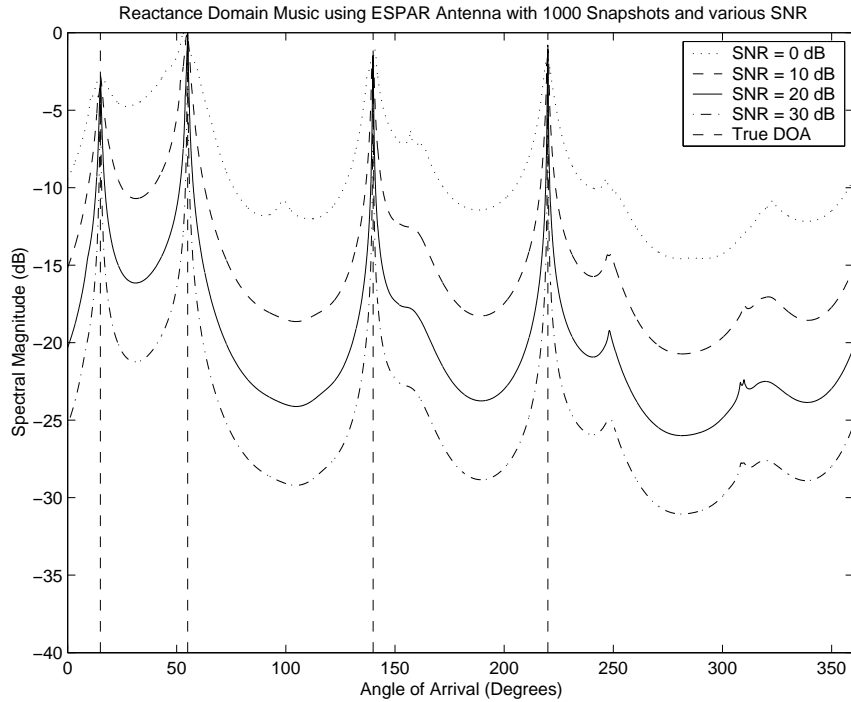


Fig. 15 Reactance MUSIC spectra for various signal-to-noise ratios for the six element ESPAR

4) 7 Element ESPAR Antenna

The results for Reactance Music algorithm are presented for an ESPAR antenna with 7 elements. The reactances used in this case were:  $X_1 = 0 -14i$ ,  $X_2 = 0 -65i$ ,  $X_3 = 0 +39i$ ,  $X_4 = 0 +17i$ ,  $X_5 = 0 +39i$ ,  $X_6 = 0 -65i$  and  $X_7 = 0 + 30i$ .

The 7 element cannot resolve more than 6 signals and it performs well even in all SNR environments.

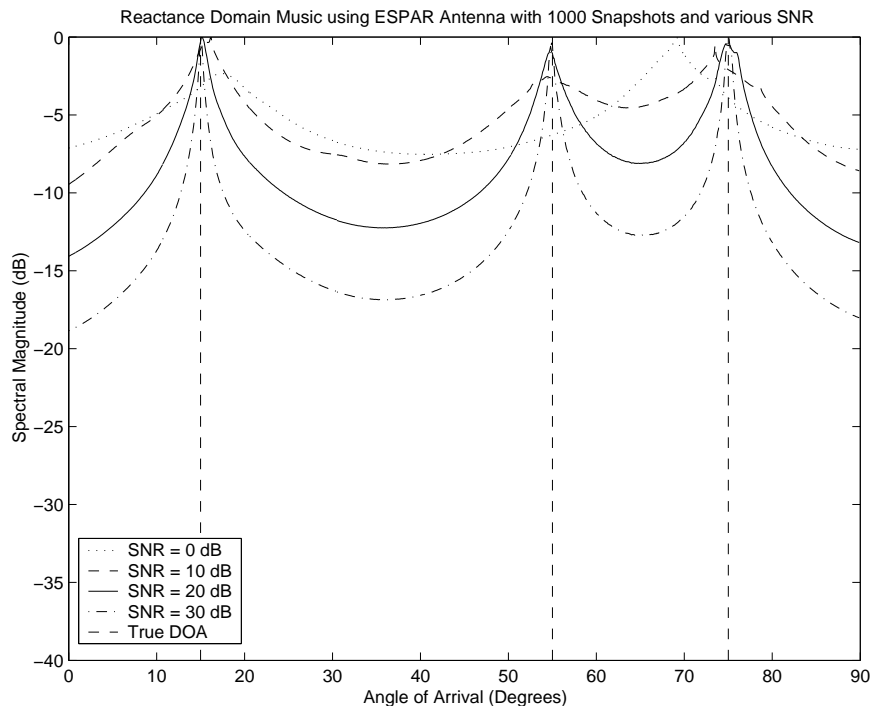


Fig. 16 Reactance MUSIC spectra for various signal-to-noise ratios for the seven element ESPAR

### 5) Comparisons of Number of Elements

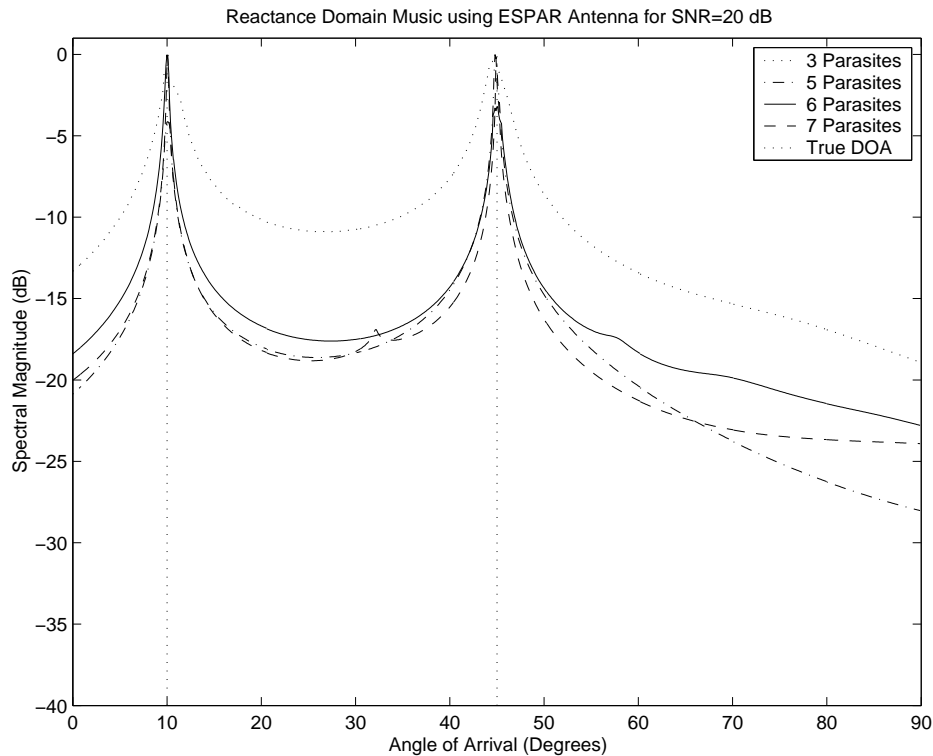


Fig. 17 Reactance MUSIC spectra for 3, 5, 6, & 7 element ESPAR antennas at SNR=20dB

From fig. 17 it can be seen that even the 3 element ESPAR is able to resolve signals clearly. However configurations with more elements provide sharper spectrum peaks. The difference in performance is negligible for 5, 6 and 7 elements.

#### D. ESPAR Diameter

Simulations were done to predict the performance of the ESPAR for various circle diameters. The goal was to determine the best configuration for this antenna. Simulations were done for the following combinations:

- 0.25  $\lambda$  Diameter
- 0.30  $\lambda$  Diameter
- 0.40  $\lambda$  Diameter
- 0.50  $\lambda$  Diameter
- 0.60  $\lambda$  Diameter
- 0.70  $\lambda$  Diameter
- 1.00  $\lambda$  Diameter

In all cases the configuration used 6 parasitic elements with the following reactance set:

$$X_1 = 0 -14i, X_2 = 0 -65i, X_3 = 0 +39i, X_4 = 0 +17i, X_5 = 0 +39i, X_6 = 0 -65i$$

The simulation frequency, load reactances and SNR are kept constant. The azimuth angle range covers 0 to 90 degrees. The results are presented using Reactance MUSIC spectra, Smith Charts and Radiation patterns.

The following figure shows MUSIC spectra for three configurations of diameter. It can be seen that  $0.5\lambda$  diameter provides the sharpest peaks.

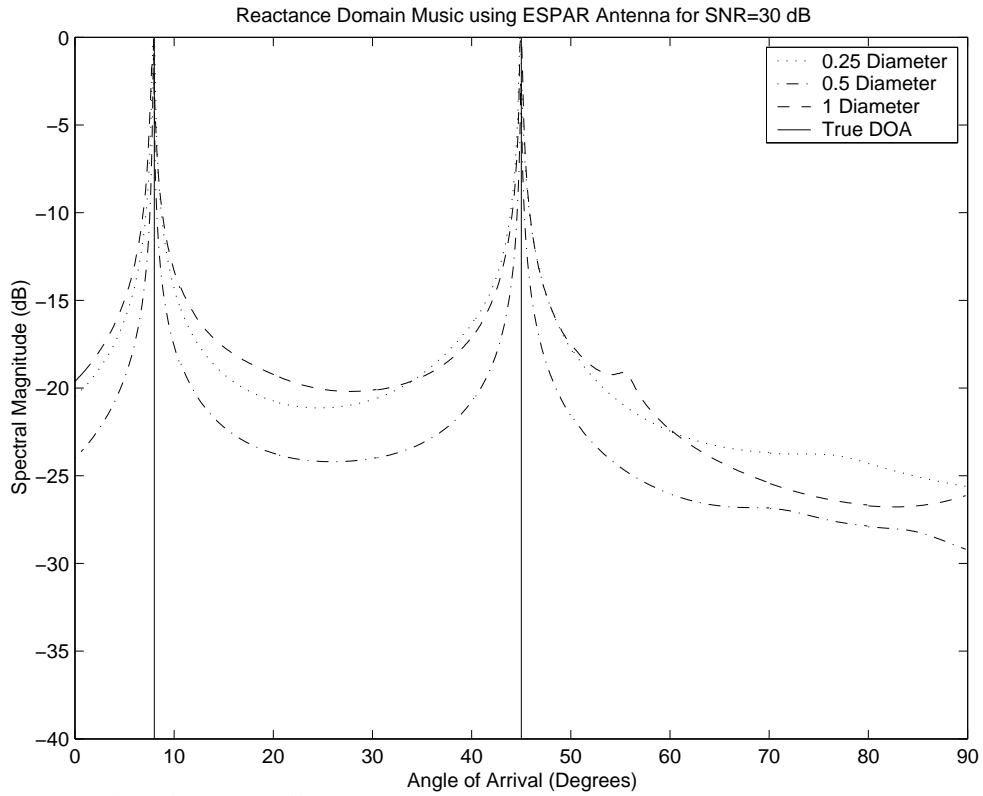


Fig. 18 Reactance MUSIC spectra for various ESPAR diameters

Fig. 19 shows that there are slight performance differences for the diameter range  $0.4\lambda - 0.6\lambda$ . Again it can be seen that  $0.5\lambda$  provides the sharpest peaks.

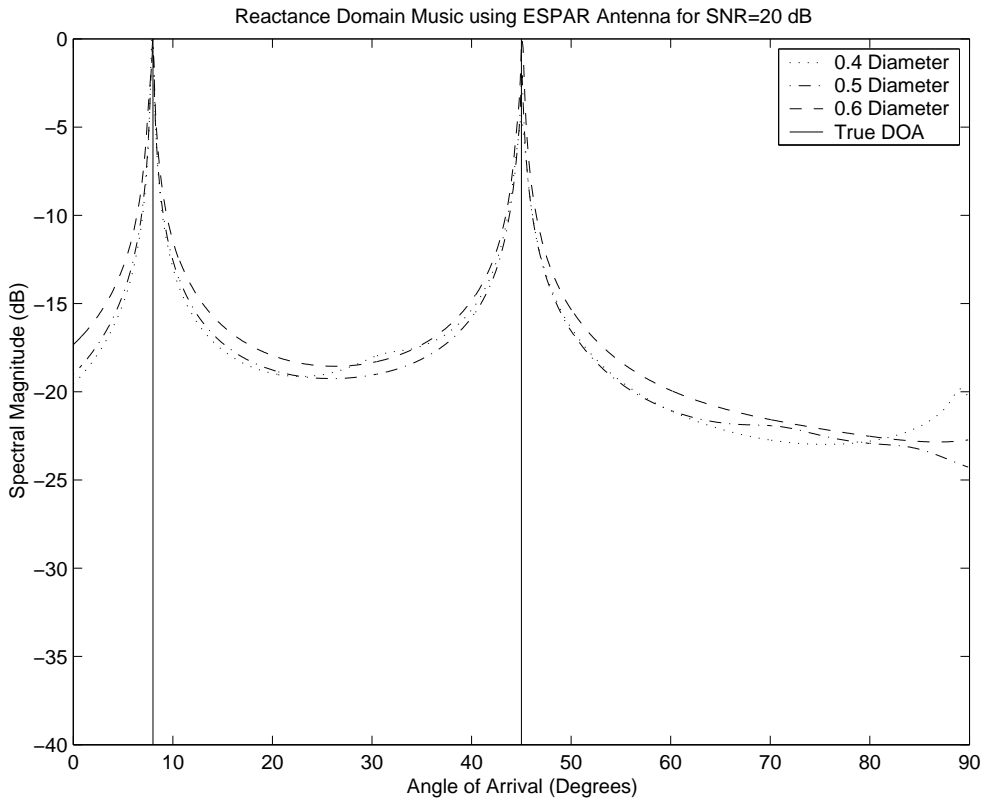


Fig. 19 Reactance MUSIC spectra for  $0.4\lambda$ ,  $0.5\lambda$  and  $0.6\lambda$  ESPAR diameters

The following Smith Chart in fig. 20 shows that the reactance increases with diameter. The impedance moves on a constant circle of reactance.

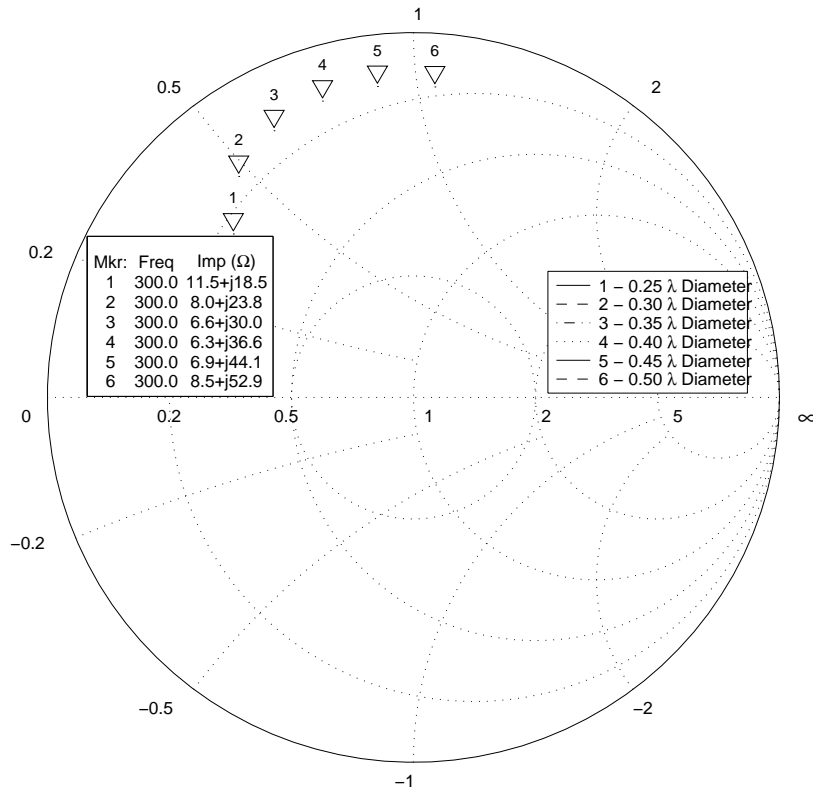


Fig. 20 Smith chart for the ESPAR of diameters 0.25 $\lambda$  - 0.5 $\lambda$

The radiation patterns in fig. 21 show that the radiation pattern has deep nulls and sharper peaks when the diameter is small while it maintains a non-uniform shape without these sharp areas at 0.5 $\lambda$ .

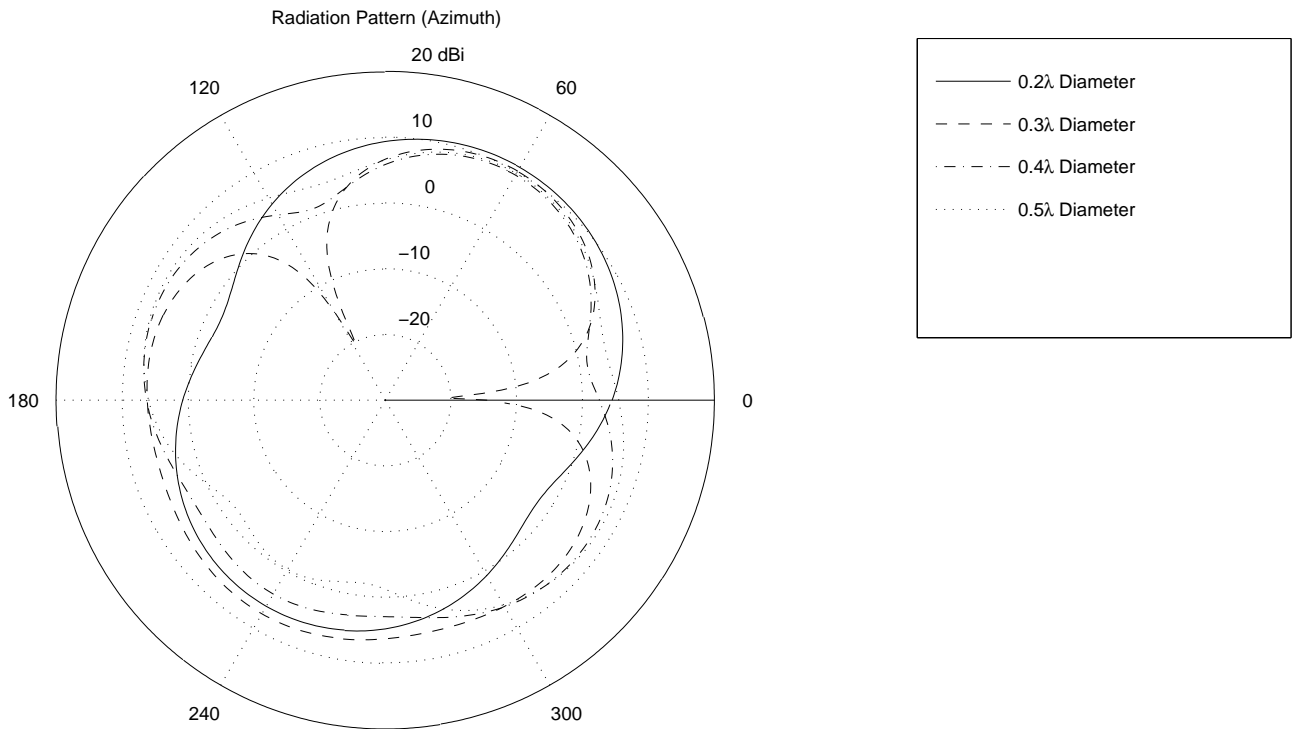


Fig. 21 Radiation patterns for 0.25 $\lambda$  to 0.5 $\lambda$  diameter ESPAR configurations

E. Reactance Music

Simulations were done to investigate the performance of the Reactance Domain MUSIC algorithm in resolving multiple signals with various ESPAR configurations.

1) Snapshots

The dependence on the number of snapshots is shown in fig. 22. It is possible to see that the more snapshots that are taken of the incoming wave, the more defined the peaks of the spectrum are.

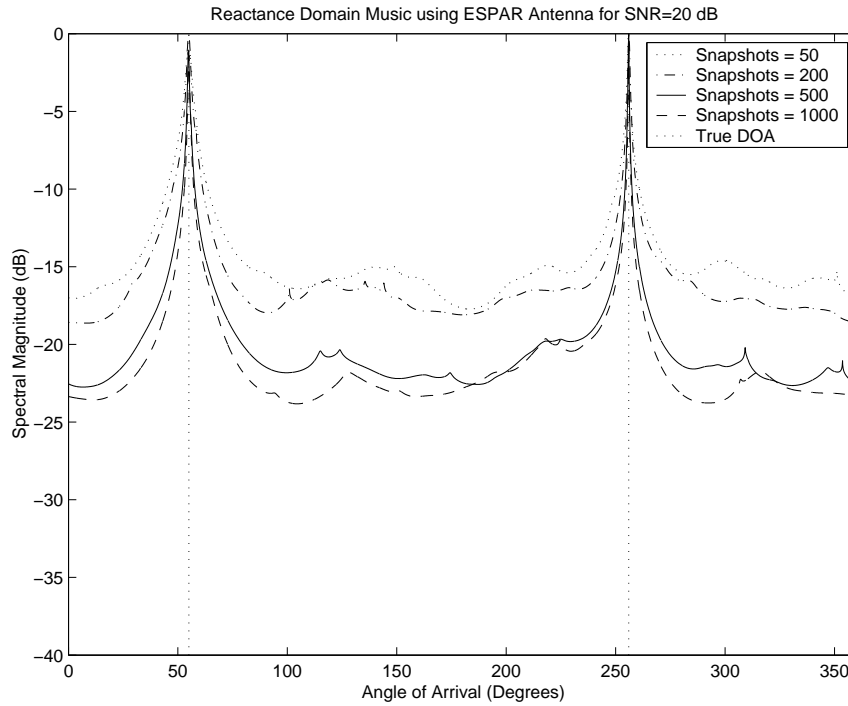


Fig. 22 Reactance MUSIC spectra resolving 2 signals at 20dB SNR for 50, 250, 500 and 1000 snapshots

The following figure shows the lower limits for numbers of snapshots. It is notable that above 50 snapshots, the algorithm produces deep maxima in the spectra that are clear to resolve.

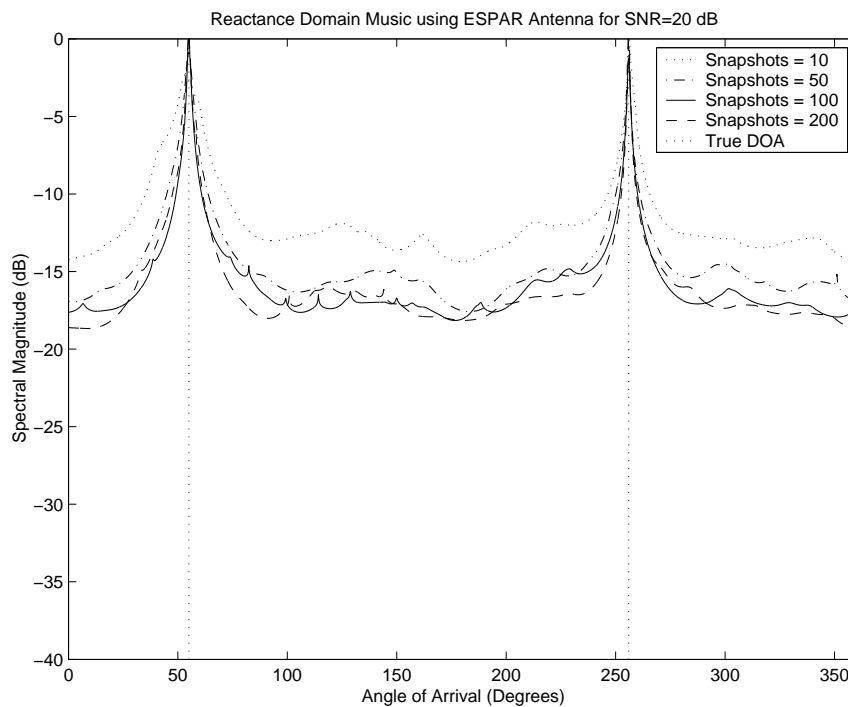


Fig. 23 Reactance MUSIC spectra resolving 2 signals at 20dB SNR for 10, 50, 100 and 200 snapshots



## 2) Signal to Noise Ratio

The following figure demonstrates the dependence on the Signal to Noise Ratio (SNR). Higher SNR produces deeper and sharper maxima in the spectrum, while lower SNR produces shallow maxima and allows for spurious peaks to enter into the spectrum making it difficult to decide if there is in fact a signal present.

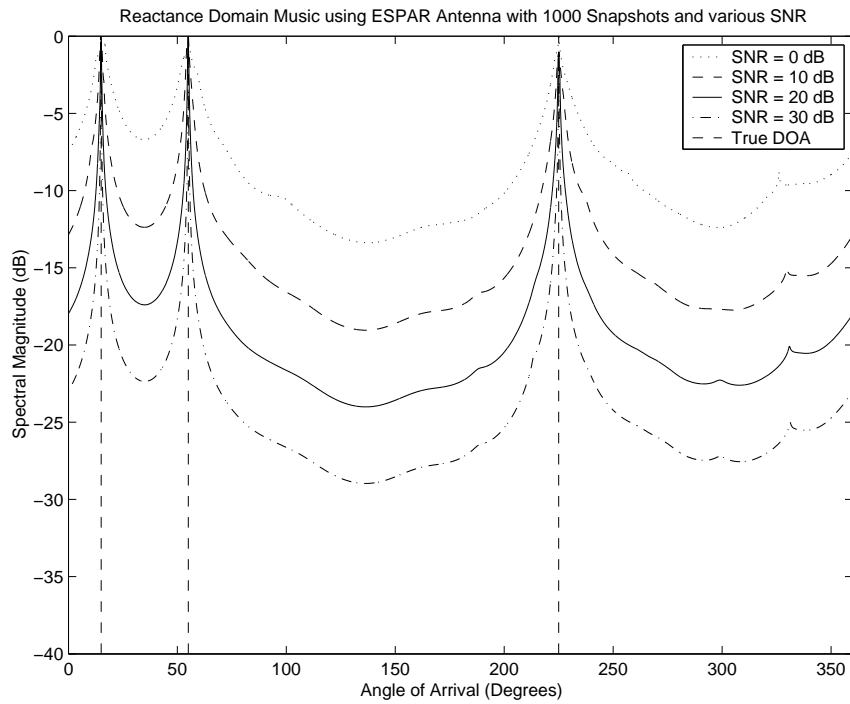


Fig. 24 Reactance MUSIC spectra for SNR of 0, 10, 20 and 30 dB

## 3) Signal Separation

Figure 25 shows that signals as close as  $1^\circ$  apart can be resolved provided that the SNR is high enough. Should the SNR fall to 20dB or 30dB, the signals will not be detectable.

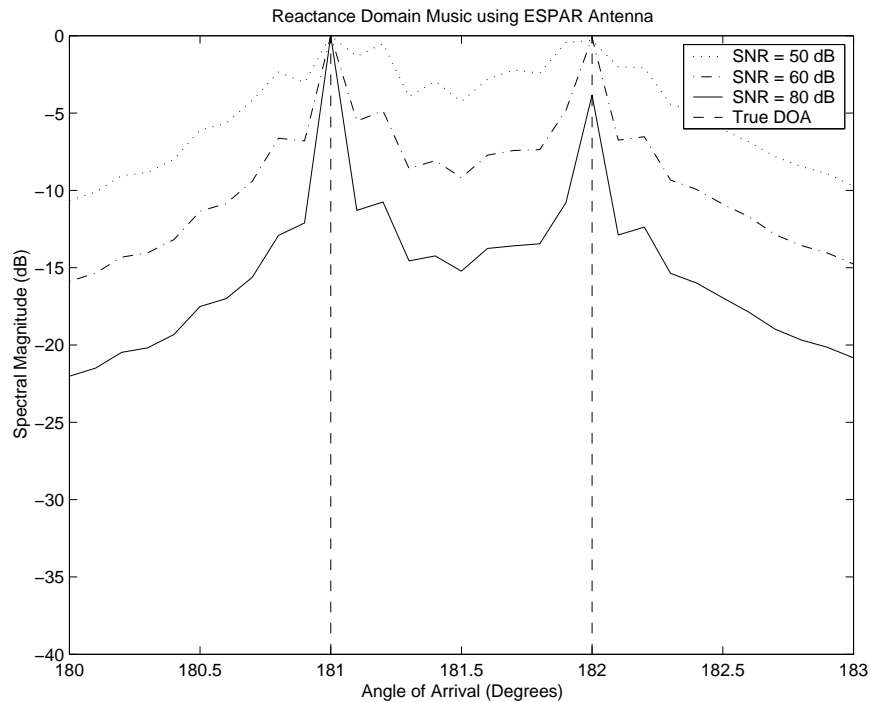


Fig. 25 Reactance MUSIC spectra with 1000 snapshots and various SNR for azimuth separation of  $1^\circ$

Signals separated by  $0.5^\circ$  were considered in the following simulation. It is clear from fig. 26 that the peaks in the spectra indicate that the signals can be resolved. This is however only possible for SNR of 60dB and above.

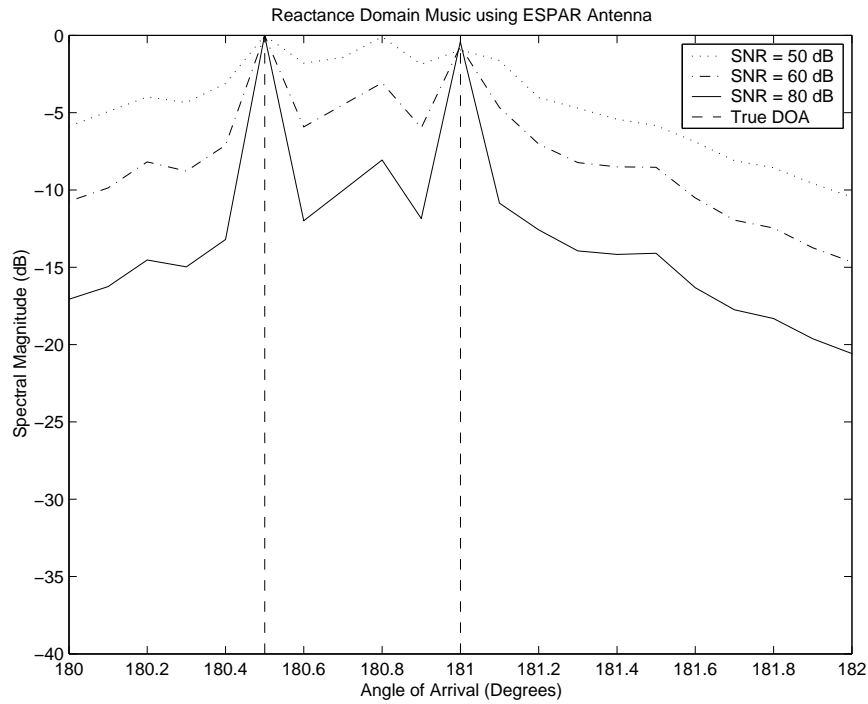


Fig. 26 Reactance MUSIC spectra with 1000 snapshots and various SNR for azimuth separation of  $0.5^\circ$

The limiting case of signal separation is shown in fig. 27. Here signals spaced  $0.2^\circ$  in azimuth are resolved with sharp peaks in the spectra.

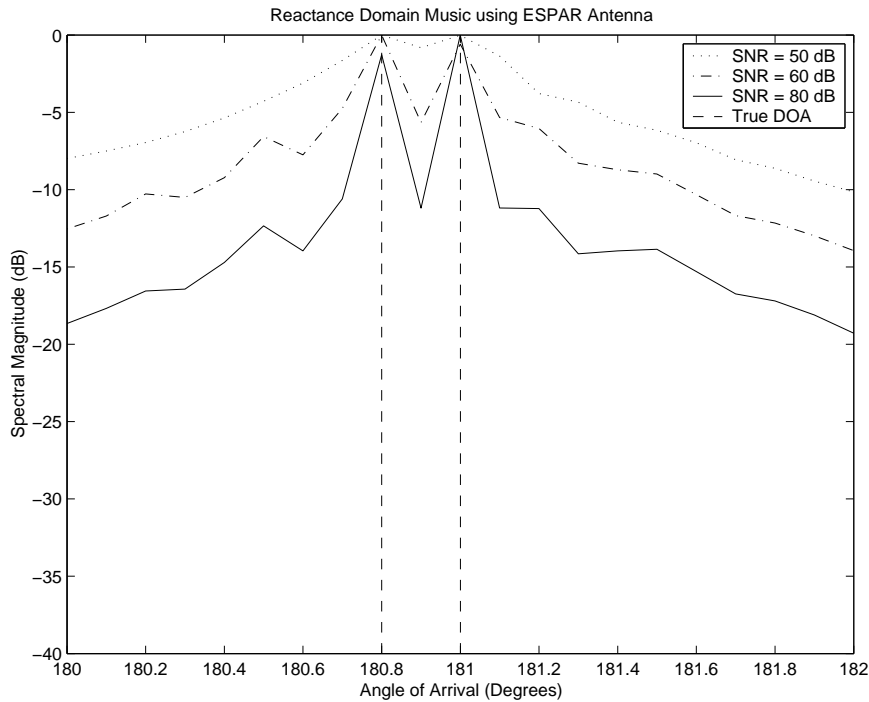


Fig. 27 Reactance MUSIC spectra with 1000 snapshots and various SNR for azimuth separation of  $0.2^\circ$

#### 4) Different Power Levels

Investigations were done to determine if the Reactance Domain MUSIC algorithm is able to resolve signals impinging on the ESPAR of various power levels. From fig. 28 it can be seen that signals as low as 25% of full power can be resolved clearly. The resulting maxima of a low powers signal are also low. This could make it difficult to detect signal amongst spurious peaks caused by random noise. In this case the 25% signal produces a peak limited in height, but is still simple to detect.

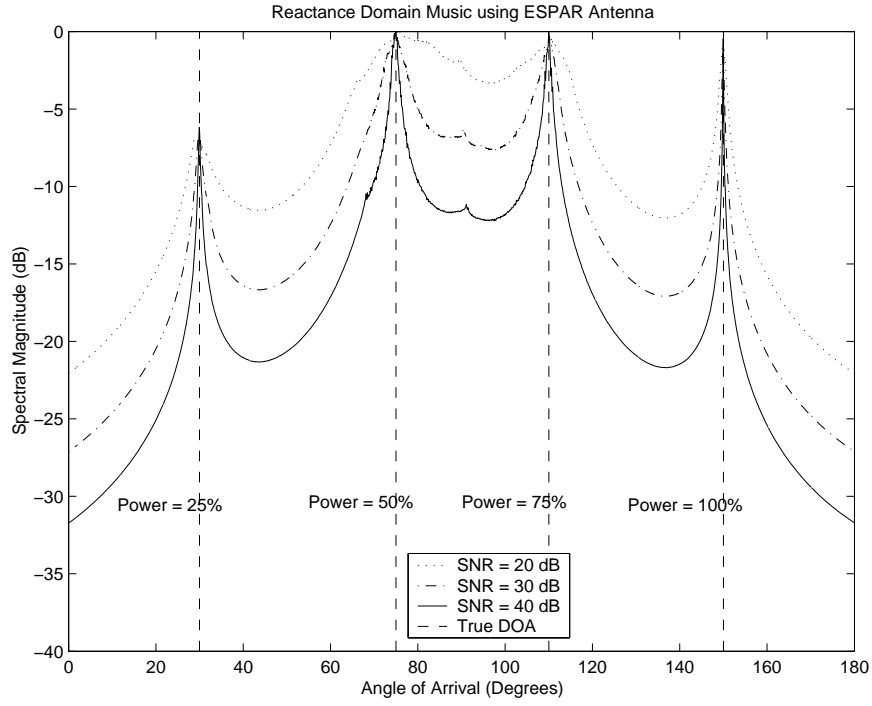


Fig. 28 Reactance MUSIC spectra for signals impinging with various power levels

5) Azimuth & Elevation Coverage

It is known that various direction finding systems have limited performance in terms of the azimuth and elevation coverage. The uniform linear array suffers ambiguity errors over  $180^\circ$  azimuth. From fig. 29 it is clear that the ESPAR antenna is capable of resolving signals equally well over full  $360^\circ$  azimuth while the elevation angle is kept constant at  $90^\circ$ .

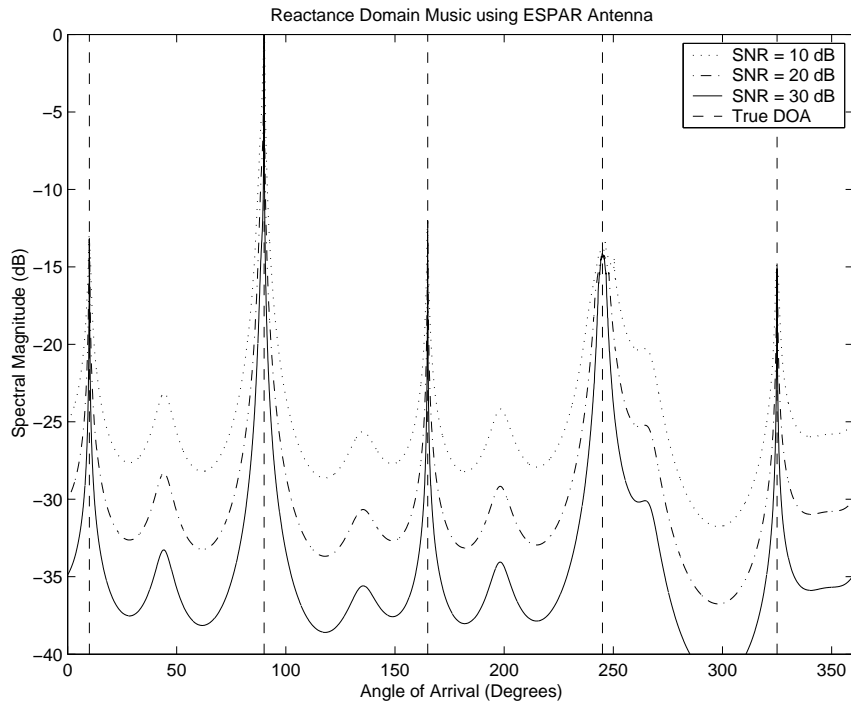


Fig. 29 Reactance MUSIC spectra with five signals dispersed over  $360^\circ$  azimuth

The following figure shows three impinging signals from elevation angles of 15°, 25°, 45° and 90°. It is clear that a signal from 15° or 25° elevation cannot be resolved, while a signal from 45° elevation produces a reduced but detectable maximum in the spectrum.

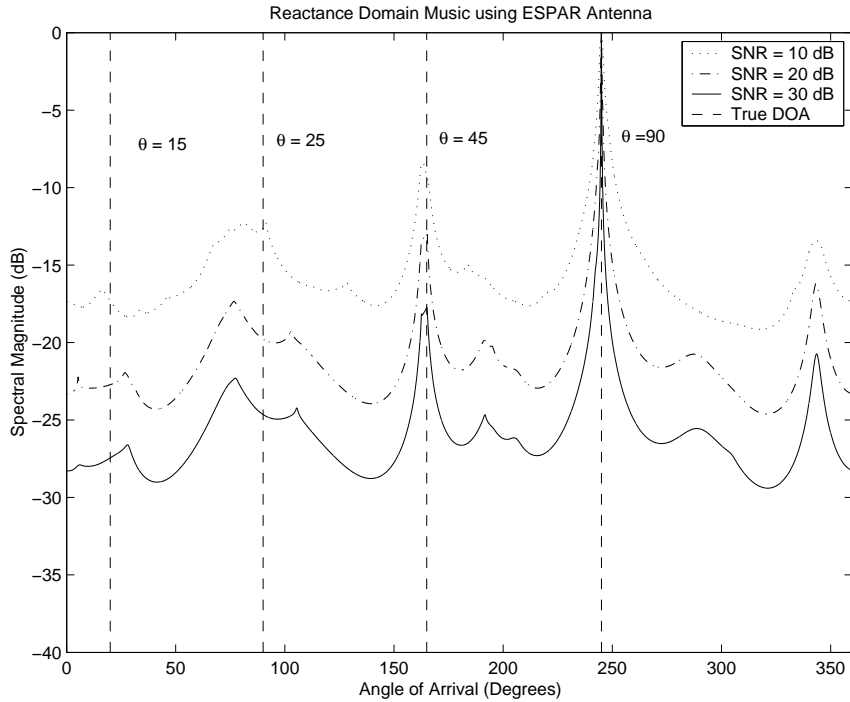


Fig. 30 Reactance MUSIC spectra for elevation angles of 15°, 25°, 45° and 90°

F. Statistical Analysis

The additive noise in the following simulation has a white Gaussian distribution with a variance of 1. Noise is generated by the Matlab Pseudo Random Number Generator. As the resulting noise depends on the state of the generator, a statistical analysis was done to determine if the MUSIC algorithm would converge to the correct azimuth direction. From fig. 31 it is clear that the algorithm will converge to the correct value. It should also be noted that at a SNR of 10dB there are many spurious peaks in the spectrum.

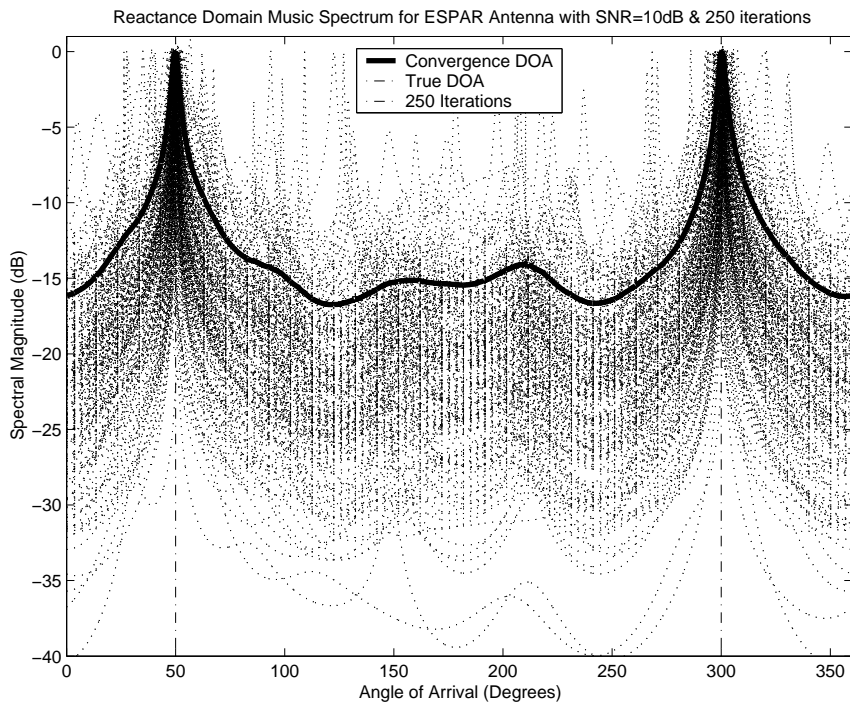


Fig. 31 Statistical analysis of Reactance MUSIC spectra with 250 iterations

### G. Load Reactances

The fifteen load sets that were used in the simulations are shown in Table V. Simulation results using these sets are shown in the following figures. In all cases the values of the reactances were selected randomly except for the Optimised set which was taken from Schlub [1] who used a genetic algorithm to determine an optimised set. Spectra are not included for reactance sets 1, 2, 3 and 8 as the directions were not able to be resolved.

TABLE V LOAD REACTANCE SETS USED FOR THE OPTIMISATION

| Set No. | Set Name     | $X_1$  | $X_2$   | $X_3$  | $X_4$   | $X_5$  | $X_6$   |
|---------|--------------|--------|---------|--------|---------|--------|---------|
| 1       | Zero         | 0      | 0       | 0      | 0       | 0      | 0       |
| 2       | Equal        | 50     | 50      | 50     | 50      | 50     | 50      |
| 3       | Ordered      | 0+ 30i | 0+ 10i  | 0+ 30i | 0+ 10i  | 0+ 30i | 0+ 10i  |
| 4       | Capacitive   | 0- 10i | 0- 60i  | 0- 30i | 0- 5i   | 0- 75i | 0- 40i  |
| 5       | Inductive    | 0+ 10i | 0+ 60i  | 0+ 30i | 0+ 5i   | 0+ 75i | 0+ 40i  |
| 6       | Max/Min      | 0      | 0+ 100i | 0      | 0- 100i | 0      | 0+ 100i |
| 7       | Optimised    | 0- 14i | 0- 65i  | 0+ 39i | 0+ 17i  | 0+ 39i | 0- 65i  |
| 8       | Real only    | 10     | 60      | 25     | 80      | 40     | 100     |
| 9       | Limited +25j | 0+ 20i | 0- 10i  | 0- 5i  | 0+ 7i   | 0- 18i | 0+ 25i  |
| 10      | Random1      | 0+ 5i  | 0+ 66i  | 0- 33i | 0+ 40i  | 0- 75i | 0+ 20i  |
| 11      | Random2      | 0+ 10i | 0- 90i  | 0+ 45i | 0- 16i  | 0+ 77i | 0- 5i   |
| 12      | Random3      | 0- 90i | 0+ 16i  | 0+ 33i | 0+ 46i  | 0- 70i | 0- 10i  |
| 13      | Random4      | 0+ 43i | 0+ 49i  | 0- 10i | 0+ 21i  | 0+ 25i | 0- 50i  |
| 14      | Random5      | 0+ 16i | 0- 60i  | 0+ 50i | 0- 50i  | 0+ 33i | 0+ 99i  |
| 15      | Random6      | 0+ 12i | 0+ 25i  | 0- 40i | 0+ 80i  | 0- 5i  | 0- 10i  |

The following figure shows the MUSIC spectrum for load reactance sets Inductive, Capacitive and MaxMin. In all three cases the directions of arrival can be clearly resolved.

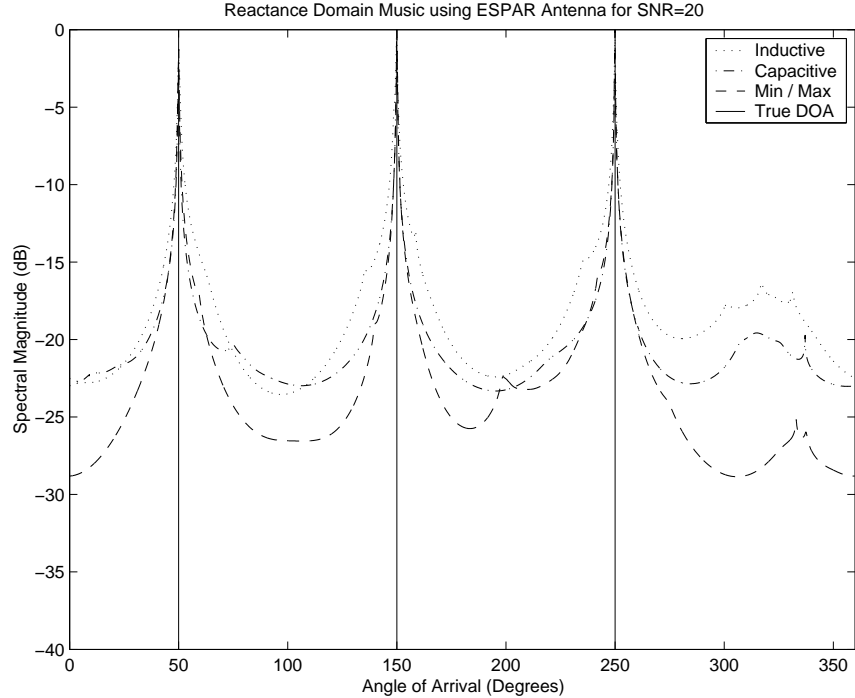


Fig. 32 Reactance MUSIC spectra for Inductive, Capacitive and MaxMin Load reactance sets

The radiation pattern for these reactance sets is shown in fig. 33. While the Capacitive set resolves the direction information well in fig. 32 it should not be employed due to the deep nulls in the radiation pattern. The deep nulls are likely to cause the desired signal to be missed.

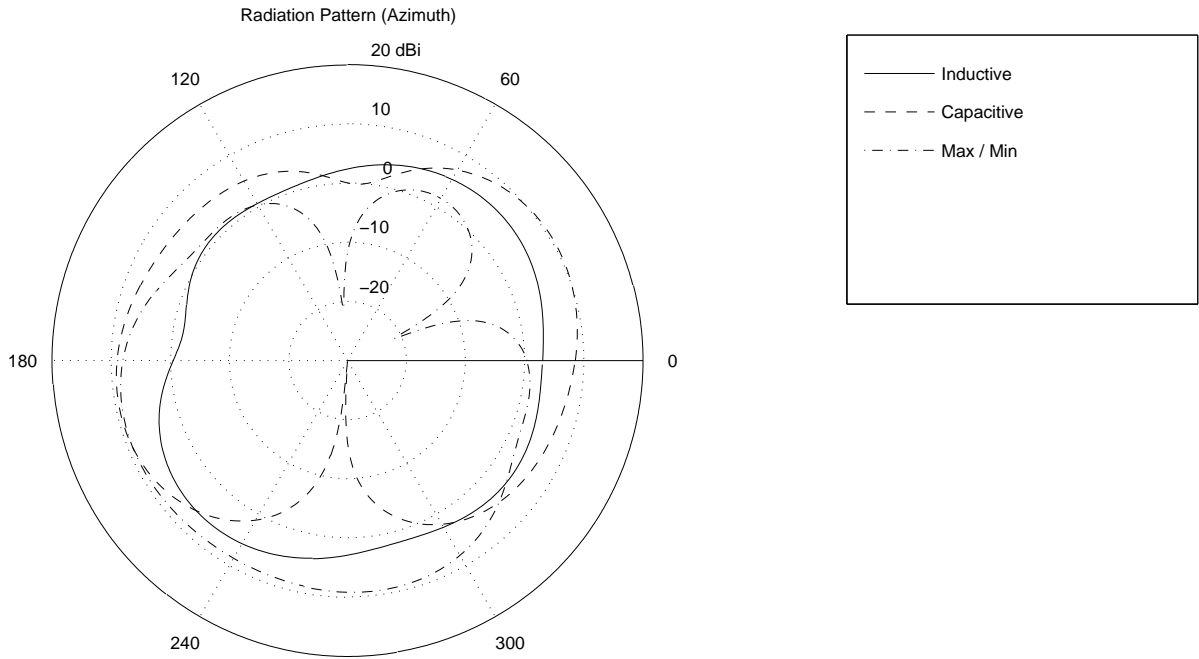


Fig. 33 Radiation pattern for load reactance sets Inductive, Capacitive and MinMax

The following figure shows the MUSIC spectrum for load reactance sets Random1, Random2 and Random3. In all three cases the directions of arrival can be clearly resolved, but Random3 produces the smoothest and deepest spectra.

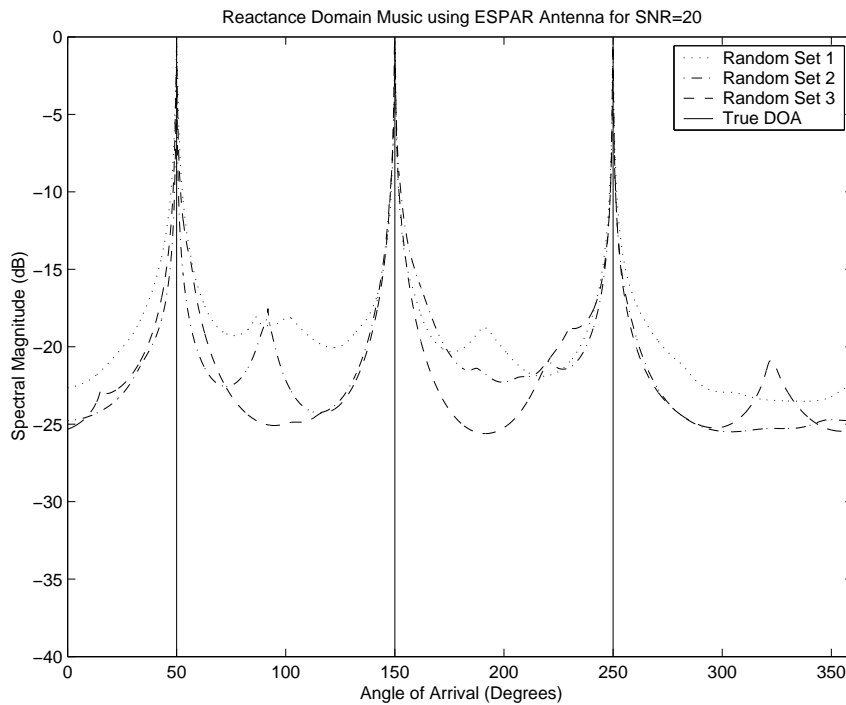


Fig. 34 Reactance MUSIC spectra for loads sets Random1, Random2 and Random3

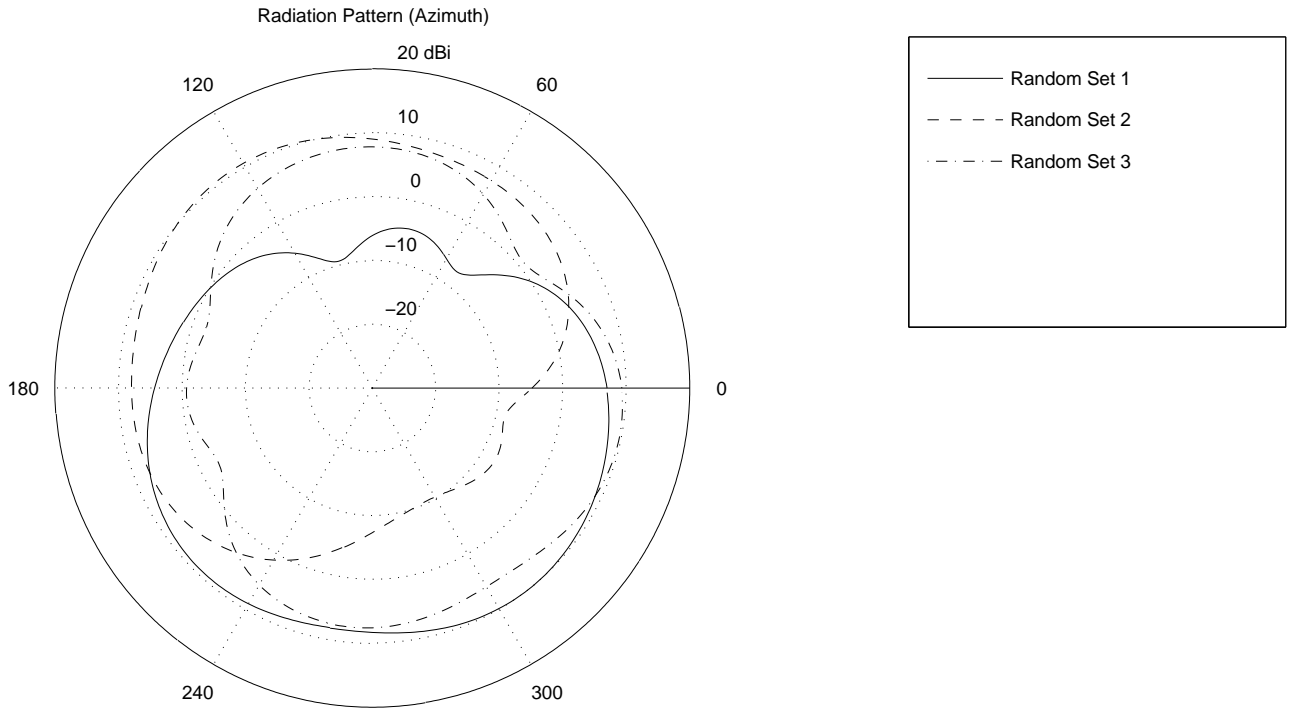


Fig. 35 Radiation pattern for load reactance sets Random1, Random2 & Random3

The following figure shows the MUSIC spectrum for load reactance sets Random4, Random5 and Random6. In all three cases the directions of arrival can be clearly resolved. The performance is comparable from all three sets.

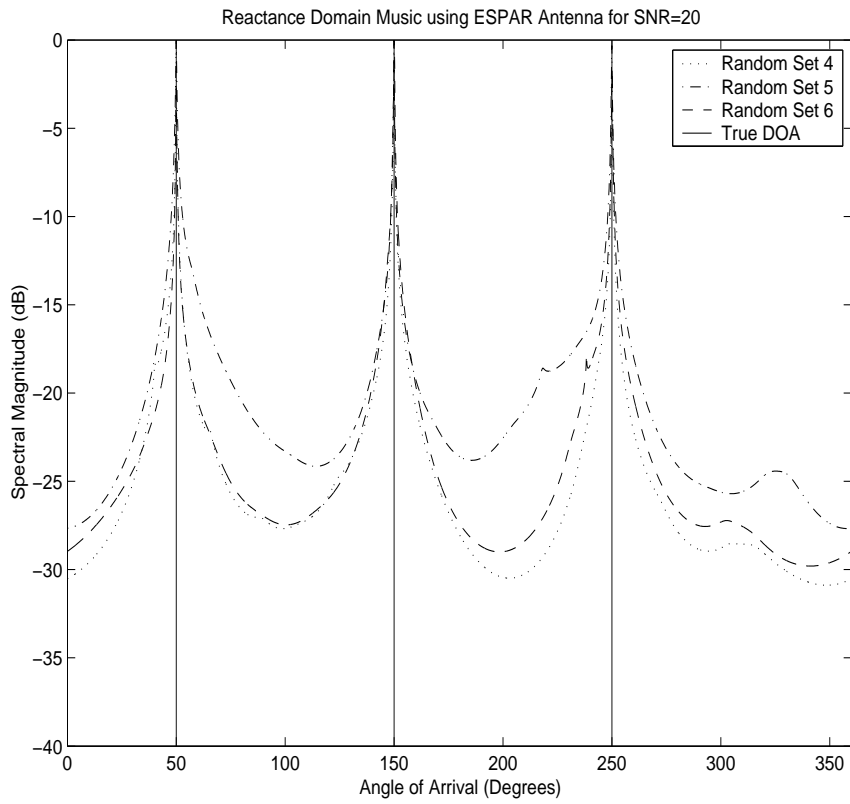


Fig. 36 Reactance MUSIC spectra for loads sets Random4, Random5 and Random6

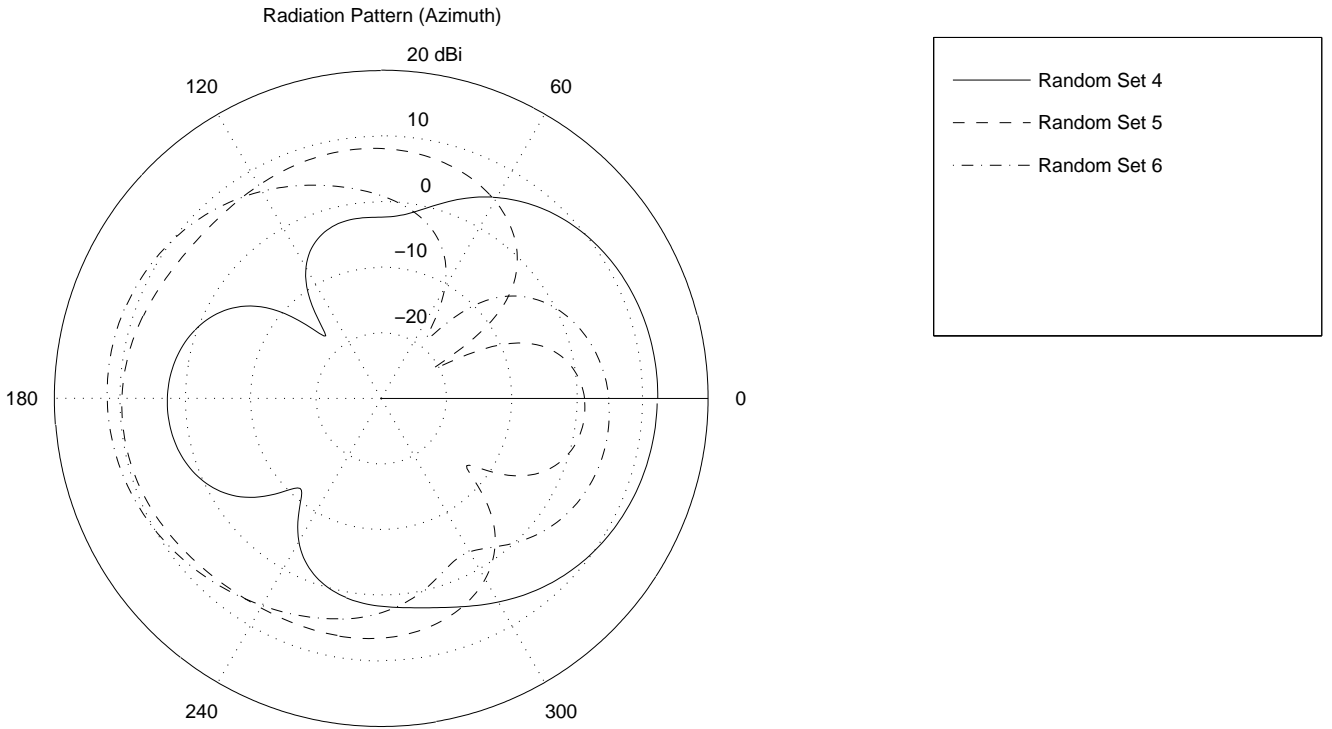


Fig. 37 Radiation pattern for load reactance sets Random4, Random5 & Random6

The following figure shows the MUSIC spectrum for load reactance sets Optimised, Random4 and Limited25. In all three cases the directions of arrival can be clearly resolved.

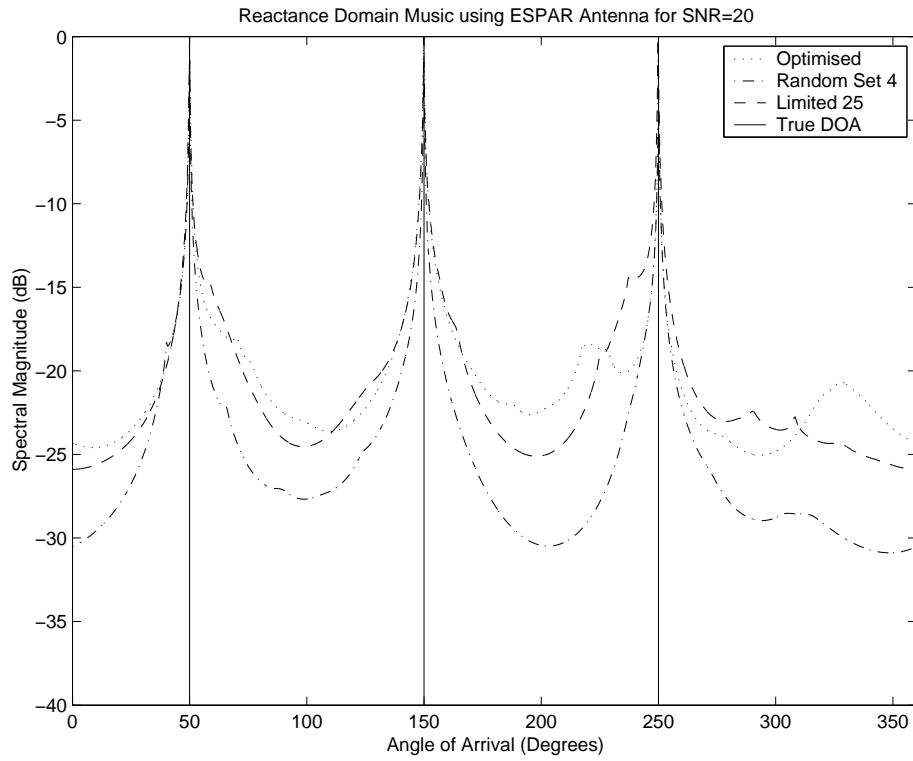


Fig. 38 Reactance MUSIC spectra for loads sets Optimised, Random4 & Limited25



In order for the Reactance MUSIC algorithm to determine the direction of arrival correctly, the radiation pattern should be asymmetrical and non-uniform so that it may be virtually rotated to recreate spatial diversity. The radiation patterns resulting from the load reactance sets are shown in fig. 39.

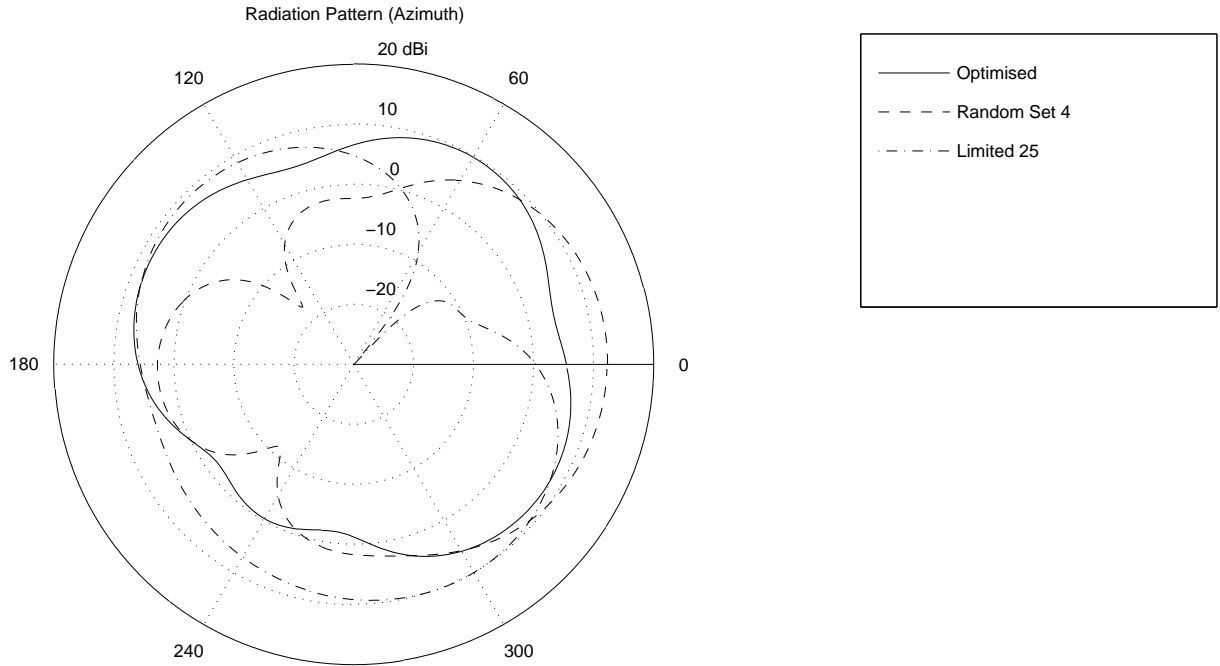


Fig. 39 Radiation pattern for load reactance set Optimised, Random4 & Limited25

Finally, the impedance bandwidth was analysed by investigating the VSWR performance for the various load reactance sets. Due to the complex structure of the ESPAR antenna it is difficult to maintain the VSWR below 5:1 for a wide bandwidth. The VSWR for reactance sets Random1, Random2, Random3 and Random4 are shown in fig. 40. It can be seen that Random3 provides a response that remains below the VSWR 5:1 for 10% of the centre frequency.

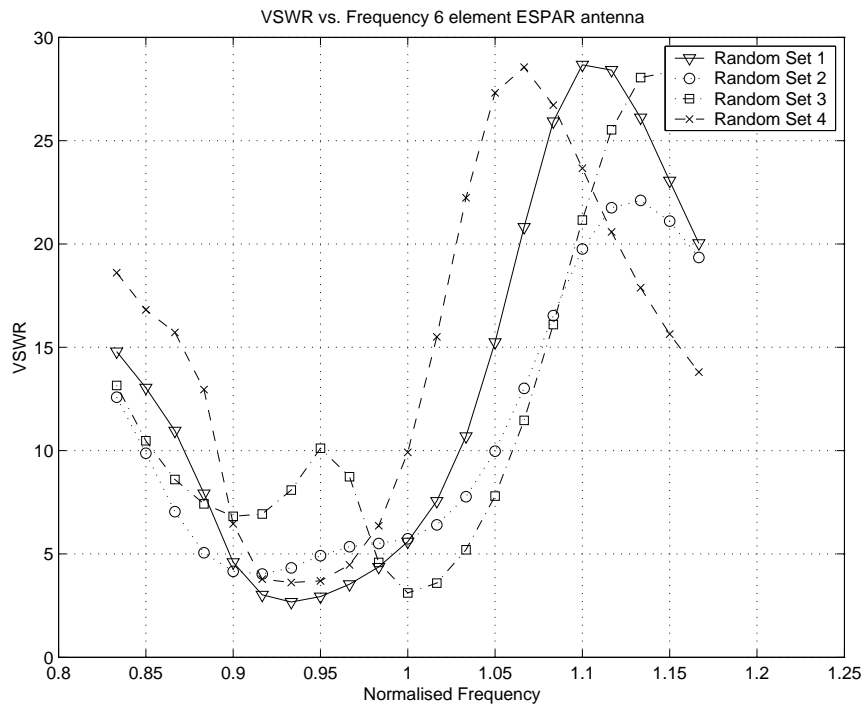


Fig. 40 VSWR response of the ESPAR antenna for reactance sets Random1, Random2, Random3 and Random4.

The VSWR for reactance sets Random4, Random5, Random6 and Optimised are shown in fig. 41. It can be seen that Random5 provides a response that remains below the VSWR 5:1 for 10% of the centre frequency. The other sets show a poor VSWR performance.

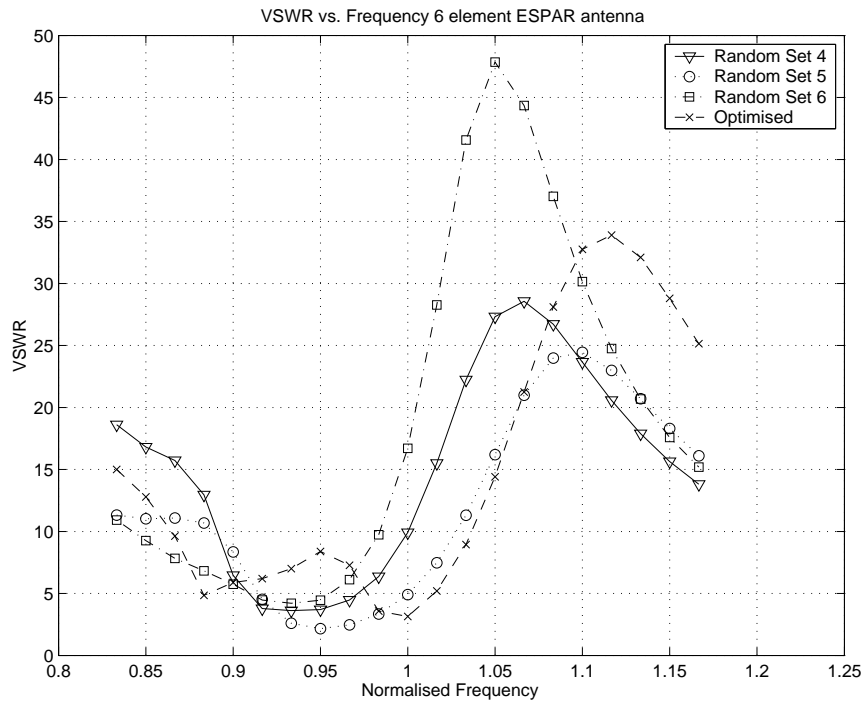


Fig. 41 VSWR response of the ESPAR antenna for reactance sets Random4, Random5, Random6 and Optimised.

Fig. 42 shows the VSWR for reactance sets Optimised, MinMax, Inductive and Capacitive. In this case it can be seen that Optimised performs the best at the centre frequency and remains below 10:1 for 15% of the centre frequency. The other sets show a poor VSWR performance.

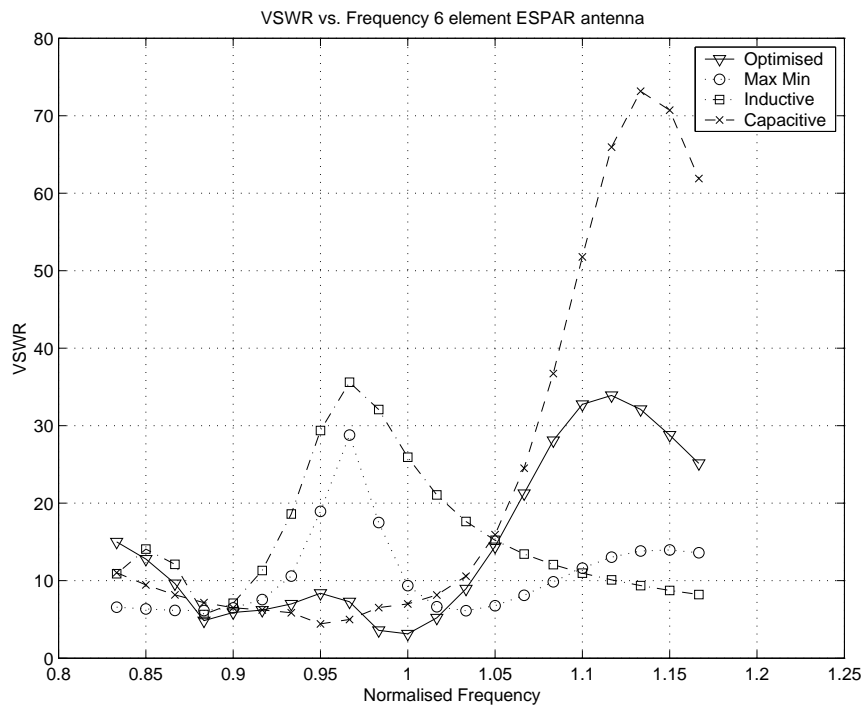


Fig. 42 VSWR response of the ESPAR antenna for reactance sets Optimised, MaxMin, Inductive and Capacitive

## *H. Conclusion*

From the above simulation results it can be seen that the best direction finding performance is gained from an ESPAR antenna with 6 parasitic elements and a diameter of  $0.5\lambda$ . The Reactance domain MUSIC algorithm used to extract the direction of arrival information performs best with more snapshots, but is capable of resolving a signal with as little as 50 snapshots of the received signal. Low signal to noise ratios produce spurious peaks in the MUSIC spectra, but even a 0dB SNR is capable of resolving the DOA. Signals as close as  $0.2^\circ$  apart in azimuth are resolved when the SNR is above 55dB. Signals of various power levels arriving simultaneously at the ESPAR are easily resolved as low as 25% of full power. Various load reactance sets were investigated for the ESPAR. It was determined that in general, a random set of reactances will be able to determine the direction of arrival but the VSWR performance will not be below 5:1 for more than 10 %bandwidth. An in depth optimization scheme such as a genetic algorithm is required to determine the best set of reactances based on DOA performance and VSWR.

## *I. References*

- [1] R.W. Schlub, "Practical Realization of Switched and Adaptive Parasitic Monopole Radiating Structures.", PhD dissertation, School of Microelectronic Engineering, Griffith University, January 2004.

# Appendix B: Uniform Linear Array and ESPAR Performance Comparison Simulations

## Abstract

A comparison between a six element uniform linear array (ULA) and a six element ESPAR antenna is presented. Simulations were done in SuperNEC and Matlab and the results are shown. The ESPAR has full azimuth coverage and performs equally well at all directions. The ULA consistently produces sharper maxima in the MUSIC spectra. The Reactance Domain MUSIC algorithm produces shallower maxima at the corresponding azimuths and is capable of resolving signals  $1^\circ$  apart at SNR of 60dB. From the simulations it can be concluded that the ESPAR offers good performance despite it only requiring a single radio receiver.

## A. Introduction

The performance of the 6 element ESPAR antenna was compared to 6 element Uniform Linear Array (ULA). Simulations were done in SuperNEC and the results are presented. The ESPAR employed the Reactance Domain MUSIC algorithm [1] while the ULA used the conventional MUSIC algorithm [2].

## B. Azimuth Coverage

The azimuth coverage was simulated for the ULA and the ESPAR. The ULA typically suffers azimuth ambiguity errors when the azimuth angle exceeds  $180^\circ$ . This can be seen in fig. 43. The ESPAR antenna has a symmetrical architecture and hence does not suffer any azimuth problems.

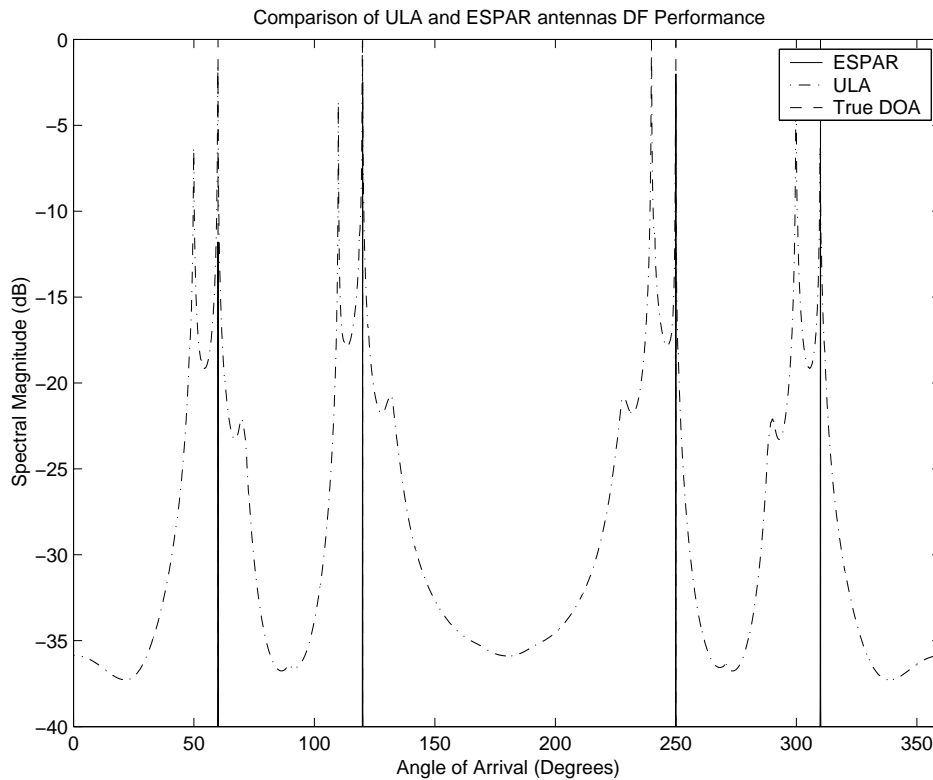


Fig. 43 Combined MUSIC spectra for 6 element ESPAR and ULA over full azimuth



#### D. Signal separation

Fig. 46 shows that the ESPAR outperforms the ULA for the case of close signal separation. In this figure signals are separated by  $1^\circ$ . Reactance MUSIC shows two distinct peaks in the spectra while conventional MUSIC produces one wide peak failing to resolve the two signals.

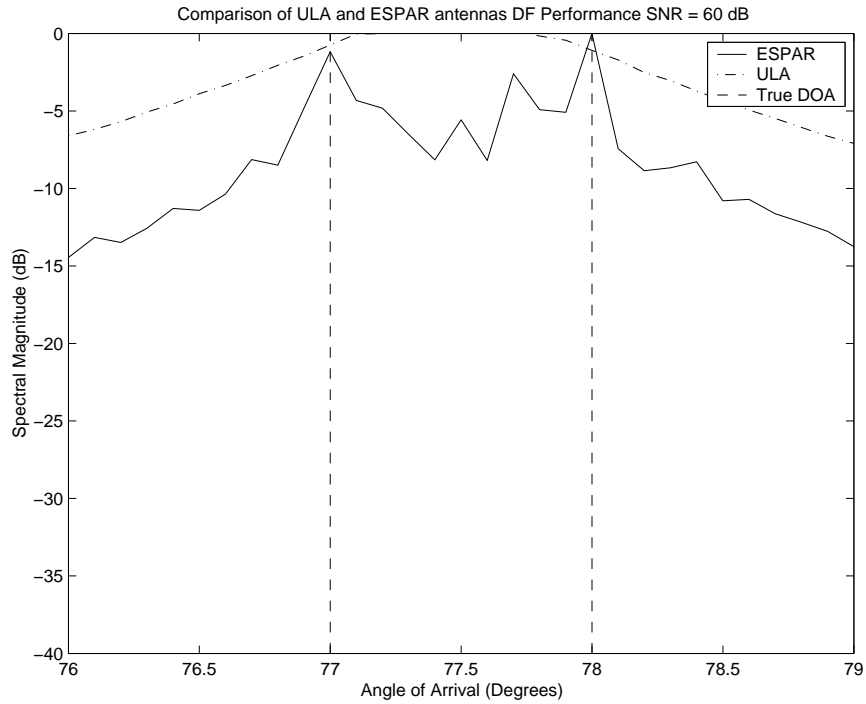


Fig. 46 Combined MUSIC spectra for ESPAR and ULA for narrow azimuth separation

#### E. Conclusion

A comparison between the ULA and the ESPAR antenna has been presented. It was shown that the ESPAR antenna competes well with the ULA in terms of performance. The ULA typically produces sharper peaks in the MUSIC spectra, while the ESPAR is capable of resolving elevated signals better. The ESPAR is also better at resolving closely spaced signals.

#### F. References

- [1] R. O. Schmidt, "Multiple emitter location and signal parameter estimation", *IEEE Trans. Antennas and Propagat.*, vol AP-34, pp. 276-280, March 1986.
- [2] Plapous, P., Cheng, J., Taillefer, E., Hirata, A., Ohira, T., "Reactance Domain MUSIC Algorithm for Electronically Steerable Parasitic Array Radiator", *IEEE Trans. Antennas Propagat.*, vol. 52, No. 12, pp3257-3263, December 2004.

# Appendix C: Software Code and Output Files

## A. Introduction

This appendix introduces the files used to simulate the Electronically Steerable Parasitic Array Radiator (ESPAR) Antenna and the Uniform Linear Array (ULA). These files were used in SuperNEC Method-of-Moments simulation software. All the files represented are stored on the CD attached to the back cover of this dissertation.

The work is presented in two main directories, \SteeringVectors and \Simulations. The content of each directory is explained below.

## B. The Simulation Files

This section details the Matlab batch files used to call SuperNEC in the simulation of the ESPAR antenna. In all files the Reactance Domain multiple signal classification (MUSIC) algorithm is used to estimate the direction information. A brief description of each file is given. Results and output files are not included as they can be generated from running the \*.m files.

The following files were used to investigate the azimuth and elevation coverage of the 6 element ESPAR antenna having diameter  $0.5\lambda$ .

\Simulations\AzimuthElevation\

- Azimuth.m* - Simulates the DF resolvability over  $360^\circ$  azimuth with elevation angles constant at  $90^\circ$
- Elevation.m* - Simulates the DF resolvability over  $360^\circ$  azimuth for elevation angles varying  $0^\circ - 90^\circ$

The following files are used for basic simulations of the ESPAR antenna.

In \Simulations\Basic\

- ESPARBasic.m* - Simulates a 6 element ESPAR antenna and the Reactance Domain MUSIC
- Joinsteer.m* - Used to join multiple \*.mat files to form a complete steering vector matrix

The following files simulate configurations of the ESPAR antenna having various diameters.

In \Simulations\Diameters\

- ESPARDiams.m* - Simulates an ESPAR antenna with a single diameter
- ESPARDiamsMulti.m* - Simulates multiple ESPAR diameters in the same file with constant number of elements
- ESPARDiamsMultiMc1.m* - Simulates multiple ESPAR diameters with multiple cases of random noise to produce a better statistical result.
- ESPARRadPatDiams.m* - Produces radiation patterns of the ESPAR for various diameters
- ESPARSmithChartDiameter.m* - Produces a Smith chart of impedances for various ESPAR diameters.

The following files are used to investigate the frequency response of the ESPAR antenna.

In \Simulations\FrequencyResponse\

- ESPARFreqResponse.m* - used to simulate the Reactance MUSIC spectra over multiple frequencies
- VSWRLoads.m* - used to investigate the VSWR over frequency for various load combinations

The following code simulates two loaded monopoles on a ground plane for various cases of spacing, loading, element length and frequency and plots the impedance output data on a Smith chart.

In \Simulations\LabTesting\

- LabTest.m* - Simulates two loaded monopoles on a ground plane and plots a Smith chart
- LabTestFreqs.m* - Simulates two loaded monopoles on a ground plane and plots a Smith chart over multiple frequencies
- LabTestLoadValue.m* - Simulates two loaded monopoles on a ground plane and plots a Smith chart for multiple loads at the base of one element
- LabTestParLength.m* - Simulates two loaded monopoles on a ground plane and plots a Smith chart for multiple lengths of monopoles
- LabTestSpacing.m* - Simulates two loaded monopoles on a ground plane and plots a Smith chart for multiple element spacing

The following files are used to simulate the 6 element ESPAR with different sets of reactances.

In *\Simulations\Loads\*

- ESPARLoads.m* - Simulates a 6 element ESPAR for one load set
- ESPARLoadsMulti.m* - Simulates a 6 element ESPAR for multiple load sets in one loop
- ESPARRadPatLoads.m* - Displays radiation patterns resulting from different load sets taken from steering vectors
- ESPARRadPatLoadsManual.m* - Displays radiation patterns for a 6 element ESPAR with manually input load values
- ESPARSmithChartElHeight.m* - Displays the impedance of the ESPAR on a Smith chart for various load sets

The following files investigate the performance of the ESPAR and Reactance MUSIC for different numbers of parasitic elements.

In *\Simulations\NumElements\*

- ESPARElements.m* - Simulates a single configuration of the ESPAR taken from the steering vector input file
- ESPARElementsMulti.m* - Simulates a multiple configurations of number of elements taken from the steering vector
- ESPARElementsSNRs.m* - Simulates a single configuration of the ESPAR for multiple SNR values
- ESPARElementsMultimcl.m* - Simulates multiple configurations for multiple cases of random noise to achieve a better statistical estimate
- ESPARElementsSNRmcl.m* - Simulates a single configuration of the ESPAR for multiple SNRs using multiple cases of noise to achieve a better statistical estimate

The following file simulate the direction finding performance when signals impinge on the ESPAR array having different power levels.

In *\Simulations\Powers\*

- Powers.m* - Estimates the Reactance MUSIC spectra for signals having various power levels

The following files investigate the resolution capability of the ESPAR and Reactance Domain MUSIC for signals arriving with small separation in azimuth.

In *\Simulations\SignalSeparation\*

- Separation.m* - Estimates Reactance MUSIC spectra for signals having azimuth separations of  $0.2^\circ$  -  $20^\circ$  for various SNR
- SepGraph.m* - Plots the dependence of Signal-to-Noise ratio versus angular separation in azimuth

The following code investigates the dependence of the Reactance Domain MUSIC algorithm on the number of snapshots used to estimate the correlation matrix.

In *\Simulations\Snapshots\*

- ESPARSnaps.m* - Estimates the Reactance Domain MUSIC spectra for various numbers of snapshots used in the formation of the data matrix

The following code plots the Reactance Domain MUSIC spectra for multiple cases of additive noise. The state of the Matlab Pseudo Random Number Generator is changed for each iteration.

In *\Simulations\Statistical\*

- ESPARStatistical.m* - Plots multiple Reactance MUSIC spectra on the same axes for multiple cases of additive noise

The following code is used to compare the performance of the 6 element ESPAR antenna and the 6 element ULA.

In *\Simulations\ULA – ESPAR\*

- Comparison.m* - Plots conventional and Reactance MUSIC spectra from the ULA and the ESPAR for comparison purposes
- ULA.m* - Simulated a 6 element ULA with conventional MUSIC to determine direction information

### C. The Steering Vectors

Steering vectors store the output response of the antenna array to every combination of azimuth direction. They are used in the Reactance Domain MUSIC algorithm to determine the direction of arrival and these files are called in the simulation files detailed above.

All steering vector files are in the Matlab matrix format (*\*.mat*) and include the following fields:



*AntennaConf:-*

- numElements* - the number of elements of the ESPAR in the simulation
- impedances* - a matrix containing the reactance set to be used to load the ESPAR elements
  - SimFreq* - the simulation frequency to be used by SuperNEC
  - ModelFreq* - the model frequency to be used by SuperNEC
  - Lambda* - the wavelength
  - monoHeight* - the height of the monopoles used to make the ESPAR
  - diameter* - the diameter of the ESPAR antenna
  - final* - a matrix used to store the array response over all the full azimuth in 0.1° increments

The following files are called to simulate the performance of ESPAR antennas of various diameter.

In *\SteeringVectors\Diameters\*

- ESPARSteerDiams0.25* - ESPAR with 6 elements and 0.25λ diameter
- ESPARSteerDiams03* - ESPAR with 6 elements and 0.3λ diameter
- ESPARSteerDiams04* - ESPAR with 6 elements and 0.4λ diameter
- ESPARSteerDiams05* - ESPAR with 6 elements and 0.5λ diameter
- ESPARSteerDiams06* - ESPAR with 6 elements and 0.6λ diameter
- ESPARSteerDiams1* - ESPAR with 6 elements and 1.0λ diameter
- GetESPARSteer* - The code used to generate these files in SuperNEC and Matlab

The following files are steering vectors for the standard configuration of the ESPAR antenna.

In *\SteeringVectors\ESPARNormal\*

- ESPARSteer.All90* - ESPAR with 6 elements and 0.5λ diameter over 90° azimuth
- ESPARSteer.All360* - ESPAR with 6 elements and 0.5λ diameter over 360° azimuth

The following steering vectors are used to simulate the 6 element ESPAR for various load sets.

In *\SteeringVectors\Loads\*

- ESPARSteerLoads25* - Reactance values limited between  $-j25 < X < +j25$
- ESPARSteerLoadsAllReal* - Reactance values randomly selected all real set 1
- ESPARSteerLoadsAllReal2* - Reactance values randomly selected all real set 2
- ESPARSteerLoadsAllReal3* - Reactance values randomly selected all real set 3
- ESPARSteerLoadsEqual* - Reactance values all equal
- ESPARSteerLoadsZero* - Reactance values all equal and zero
- ESPARSteerLoadsHiLo* - Reactance values randomly selected with maximum values 0, +j100, -j100
- ESPARSteerLoadsNeg* - Reactance values randomly selected but only capacitive
- ESPARSteerLoadsPos* - Reactance values randomly selected but only inductive
- ESPARSteerLoadsRnd1* - Reactance values randomly selected capacitive and inductive set 1
- ESPARSteerLoadsRnd2* - Reactance values randomly selected capacitive and inductive set 2
- ESPARSteerLoadsRnd3* - Reactance values randomly selected capacitive and inductive set 3
- ESPARSteerLoadsRnd4* - Reactance values randomly selected capacitive and inductive set 4
- ESPARSteerLoadsRnd5* - Reactance values randomly selected capacitive and inductive set 5
- ESPARSteerLoadsRnd6* - Reactance values randomly selected capacitive and inductive set 6
- GetESPARSteerAllLoads* - Matlab code used to generate the above steering vectors

The following steering vectors are used to simulate ESPAR configurations of various numbers of elements

In *\SteeringVectors\NumElements\*

- ESPARsteer3El* - Steering vector for 3 element ESPAR
- ESPARsteer5El* - Steering vector for 5 element ESPAR
- ESPARsteer6El* - Steering vector for 6 element ESPAR
- ESPARsteer7El* - Steering vector for 7 element ESPAR
- ESPARsteer10El* - Steering vector for 10 element ESPAR
- GetESPARSteerElements* - Matlab code used to generate the above steering vectors

The following steering vectors are for various combinations of the Uniform Linear Array.

In *\SteeringVectors\ULASteer\*

*ULA3Steer* - Steering vector for the 3 element ULA

*ULA5Steer* - Steering vector for the 5 element ULA

*ULA6Steer* - Steering vector for the 6 element ULA

*ULA7Steer* - Steering vector for the 7 element ULA

*ULA9Steer* - Steering vector for the 9 element ULA

#### *D. Conclusion*

The files used to simulate the performance of the ESPAR antenna and Reactance Domain MUSIC algorithm were presented. A brief description of the purpose of each file as well as its location was given. The Matlab and SuperNEC files are stored on the attached CD.